Girase *et al. Energy Mater.* **2025**, *5*, 500132
DOI: 10.20517/energymater.2025.14

Energy Materials

Review

Open Access

Check for updates

Recent advances in diketopyrrolopyrrole (DPP) based next-generation thermoelectric materials: an overview

Jaipal Devesing Girase, In-Chan Kim, Yun-Hi Kim*

Department of Chemistry and RIMA, Gyeongsang National University, Jinju 52828, Republic of Korea.

***Correspondence to:** Prof. Yun-Hi Kim, Department of Chemistry and RIMA, Gyeongsang National University, Jinju-dero 501, Jinju 52828, Republic of Korea. E-mail: ykim@gnu.ac.kr

How to cite this article: Girase, J. D.; Kim, I. C.; Kim, Y. H. Recent advances in diketopyrrolopyrrole (DPP) based next-generation thermoelectric materials: an overview. *Energy Mater.* **2025**, *5*, 500132. https://dx.doi.org/10.20517/energymater.2025.14

Received: 17 Jan 2025 **First Decision:** 13 Mar 2025 **Revised:** 21 Apr 2025 **Accepted:** 14 May 2025 **Published:** 2 Jul 2025

Academic Editor: Yuping Wu **Copy Editor:** Ping Zhang **Production Editor:** Ping Zhang

Abstract

The imminent global energy crisis and the growing global demand for electricity, which require the development of alternative energy conversion technologies such as organic thermoelectrics, have attracted much attention from the scientific community due to their capability to convert low-grade waste heat into electrical energy. In the last decades, p-type and n-type thermoelectric polymers have been studied extensively and have achieved significant progress in thermoelectrics. In particular, diketopyrrolopyrrole (DPP)-based thermoelectric materials have gained much attention from researchers due to their unique structural properties. This review discusses potential of DPP-based thermoelectric materials and explores recent progress on DPP-based p-type and n-type (which are relatively underexplored) thermoelectric polymers in detail, which involved the structure-property relationship, doping strategies, morphology control, and the impact of molecular design, including noncovalent interactions, backbone engineering, and dopant-polymer compatibility on thermoelectric performance of DPP-based materials and new strategies that will empower the rational design of next-generation polymeric materials for thermoelectric applications.

Keywords: Thermoelectric materials, diketopyrrolopyrrole, p-type, n-type, organic electronics

INTRODUCTION

The combustion of fossil fuels provides almost 90% of the power generated by heat engines globally.

However, the world's fast-growing demand for electricity cannot be met by fossil fuel technologies. Therefore, an urgent and essential need to develop alternative energy conversion technologies to meet the energy requirement challenge[1]. However, most renewable energy conversion devices have fundamental limitations on their maximum conversion efficiency, which is at the best less than 40%, with a significant part of that energy dissipated into the environment as heat[2]. Therefore, to address global environmental challenges and provide new opportunities for the usage of renewable energy resources, it is imperative to develop novel technologies with higher energy conversion efficiency and less waste heat. Recently, thermoelectric (TE) and photovoltaic (PV) technologies have emerged as two viable clean, sustainable energy conversion methods to address the energy crisis from an environmental and sustainable standpoint.

Significant progress has been achieved in the development of PV materials over the past ten years, but the research in the field of TE is still behind. Unlike photovoltaic techniques, TE technology has shown remarkable performance, as TE devices rely not only on solar energy but also on various heat sources, including body heat, which is a promising and alternative energy source for the future[3]. TE materials hold immense promise for powering a wide range of low-power technologies due to their ability to convert waste heat into electricity. One of the most attractive features of TE generators (TEGs) is their scalability and maintenance-free operation, making them ideal for small-scale and remote applications. This makes them excellent candidates for portable and wearable electronics. Additionally, TEGs are increasingly used to power low-energy devices such as radiator valves (Micropelt), wireless sensor nodes[4], and industrial monitoring systems[5]. In the biomedical field, TE materials are particularly valuable for powering biosensors and implants by harvesting body heat[6,7], thus eliminating the need for external power sources. Beyond healthcare, TEGs are beneficial in environments where solar energy harvesting is not viable, such as in mines, pipelines, and aircraft. In such critical or hazardous zones, TE-based sensors offer reliable solutions for fire detection, homeland security, and environmental monitoring[8,9].

Traditional TE devices are generally based on inorganic materials due to their superior TE performances and stability over organic materials. The inorganic materials such as lead telluride (PbTe)[10], bismuth telluride (Bi2Te3)[11], silicon-germanium (SiGe)[12] and tin selenide (SnSe)[13] are extensively studied, where the ZT value (dimensionless merit figure) reaches to 2.6[14-17]. On the downside, many in organic semiconductor (OSC) materials have certain disadvantages inherent to the material, such as scarcity, toxic nature, inadequate processability, high thermal conductivity, and high manufacturing cost. In the recent years, research on carbon nanotube (CNT)-based are promising TE materials. Single-walled CNTs (SWCNTs) are highly promising for thermoelectrics due to their high conductivity, ease of doping, and surface functionalization. Their charge carrier type and density can be tuned through chemical doping, though stable n-type doping remains a challenge. Forming CNT-based composites with organic or inorganic materials enhances TE performance by combining high conductivity, improved Seebeck coefficient (S), and low thermal conductivity (κ)[18,19]. On the other hand, OSCs have been neglected for decades because of their low energy conversion efficiency and potential bad thermal stability, but they are potential candidates for the conversion of low-grade thermal energy into useful electricity, as they possess low-cost, lightweight, and mechanically flexible properties compared to classical in OSCs[20]. Over the past several decades, extensive research has been dedicated to the development and modification of organic polymers and molecules with promising performance capabilities for use as TE materials[21]. Figure 1 demonstrates an increase in the number of research publications conducted in TE (keyword as thermoelectric polymer) which shows the significant efforts that have been made in the field of TE. Despite the current challenge presented by the low κ value of polymers, which remains an ongoing issue that researchers are striving to overcome, there have been many reports of organic TE materials exhibiting ZT values greater than 1, attributed to their advantageous traits of high electrical conductivities along with

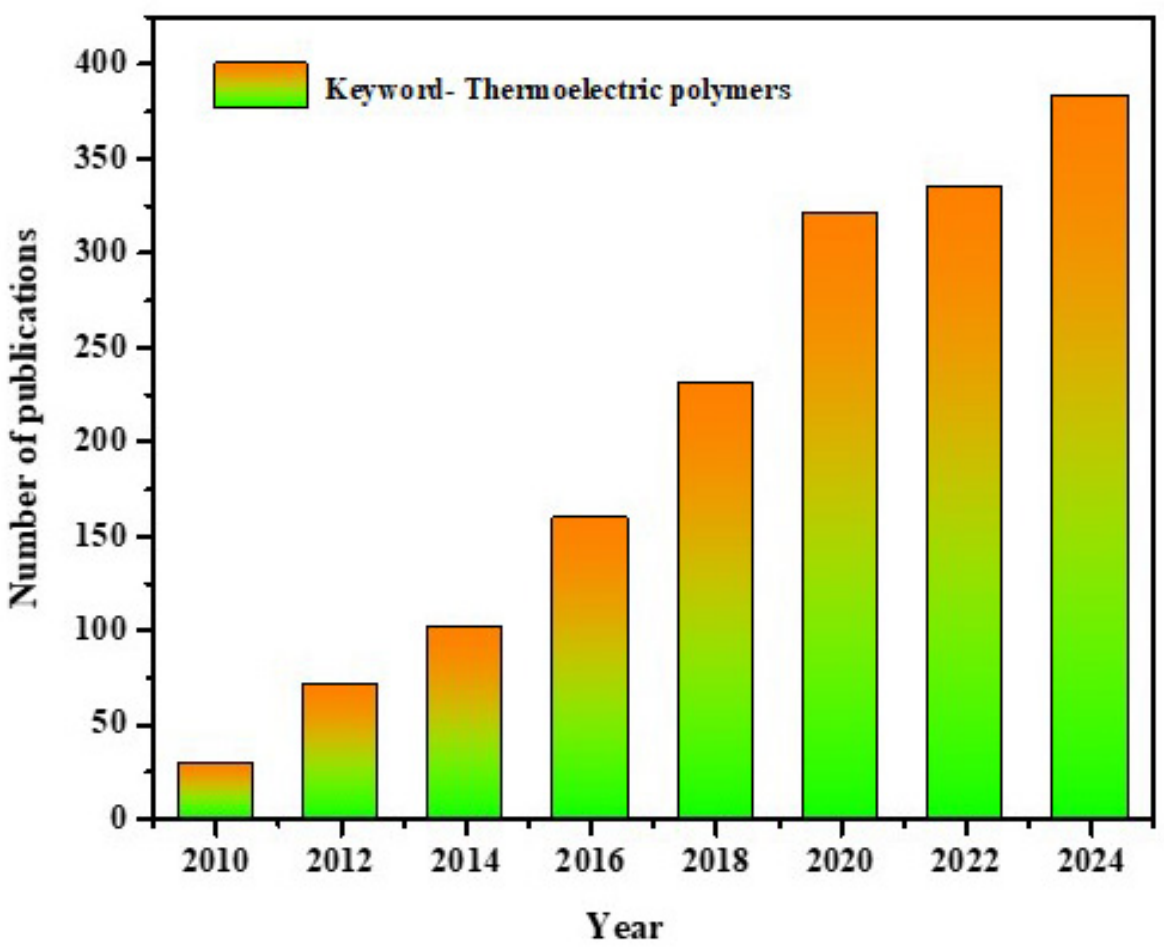

Figure 1. Trend in the number of publications related to "thermoelectric polymers" over the past decades, based on data from the Web of Science.

impressive power factor (PF)[14,22].

The most common organic materials showing TE properties are conducting polymer (CP) such as poly(3,4-ethylenedioxythiophene (PEDOT), polypyrrole (PPy), and polyaniline (PANI). These materials are considered as the most promising candidates for the TE application due to their excellent features, including low bandgap energy, high electrical conductivity (σ), thermal stability, light weight, structurally stable backbone, and ease of processing. Extensive research has been carried out on the p-type TE OSCs as these materials are mainly utilized as one of the legs in the TE devices[23-26]. However, these materials often face limitations such as hygroscopicity and insulating counter ions in PEDOT derivatives, solubility and poor air stability, processability, tunability of their structural and electronic properties, low S, and high κ, which significantly hinders their efficiency in converting thermal energy into electricity[22].

Recently, diketopyrrolopyrrole (DPP)-based polymers attracted much attention in the field of OSCs such as OSCs[27], organic field-effect transistor (OFETs)[28-31], organic light emitting diodes[32] Organic memory devices[33-35], chemical sensors[36-38], photodetectors[39,40], and light-emitting electrochemical cells[41]. The keen interest of DPP derivatives is due to their attractive features such as low production cost, wide optical

absorption, exceptionally high photochemical stability, high thermal stability, functionalized groups, and tunable semiconductivity, *etc.*[42]. Numerous DPP derivatives that have been reported in studies are either small molecules or polymers that exhibit exceptional power conversion efficiency (PCE) or high charge-carrier mobility in organic solar cell and OFETs[28,29,43-47]. It has been more than two decades since several reviews on DPP-based materials have been reported. Nonetheless, most of these reviews concentrate on the sensing, synthesis, imaging and optoelectronic applications of small molecules and conjugated polymers based on DPP[48-54]. An extensive review of the DPP-based derivatives of their TE application is still lacking.

DPP-based TE materials offer several advantages over conventional TE polymeric materials. DPP units possess a rigid, planar structure that facilitates strong π-π stacking interaction between polymer chains, leading to high charge carrier mobility and, consequently, enhanced σ[55]. Additionally, the electronic properties of DPP polymers can be readily tuned through chemical modifications, such as varying the side chains, incorporating electron-donating/withdrawing groups, and copolymerization with other monomers[56] as shown in Figure 2. Furthermore, many DPP polymers exhibit excellent thermal stability and can be processed using solution-based techniques, enabling the fabrication of flexible and low-cost TE devices.

The main objective of this review is to give a comprehensive overview of recent advancements in the TE materials, mainly focused on DPP-based donor-acceptor p-type and n-type copolymers. More specifically, the structure-property relationship, along with the strategies we have explored to enhance performance. Furthermore, we will introduce results and comparisons of different strategies aimed at improving TE performance, providing a comprehensive overview of achievements and ongoing challenges in this exciting field.

THEORY OF THERMOELECTRIC

The intrinsic property of materials to generate power from heat truly opens up the potential to harvest low-grade waste heat and convert it to electricity based on the Seebeck effect as shown in Figure 3A[57]. This effect was observed by the German scientist Thomas J. Seebeck in 1821, and it can find wide applicability in energy conversion[58,59]. The working principle of the TE energy-harvesting mechanism, if a temperature gradient (ΔT) is supplied, an electrostatic potential ΔV will be developed since the charge carriers-electrons for n-type materials or holes for p-type materials-will diffuse from the hot end to the cold end[60]. Similarly, TE materials can also transform electrical energy into thermal energy based on the Peltier effect, as shown in Figure 3B; this effect is the reverse of the Seebeck effect. This effect was discovered a few years later in 1834 by French scientist Jean Charles Athanase Peltier. He noticed that an electric current flowing through a junction of different materials transfers heat to or from that junction[61,62].

The energy conversion efficiency of TE materials is generally determined by using the dimensionless figure-of-merit (ZT) that is given by[63-65]

$$ZT = \frac{S^2\sigma}{k}T \quad (1)$$

Where S is the Seebeck coefficient, σ is the electrical conductivity, κ is the thermal conductivity, and T is the working temperature. From Equation (1), a higher S, higher σ, and lower k can therefore result in better TE performance. Materials with intrinsically high ZT are rare, nevertheless, because these three factors (S, σ, and k) are highly interdependent in most of the materials[66]. However, the intrinsic problems arise from the determination of κ for organic-based TE materials compared to that of inorganic materials; the performance

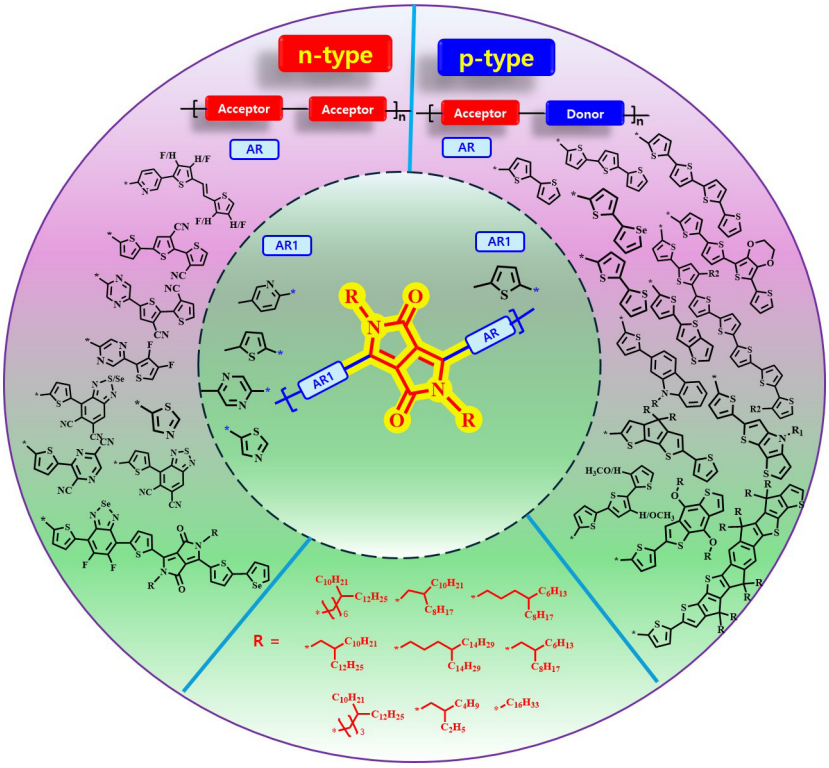

Figure 2. Schematic representation of the DPP central unit, flanked by structural moieties tailored for n-type (left) and p-type (right) thermoelectric materials. DPP: Diketopyrrolopyrrole.

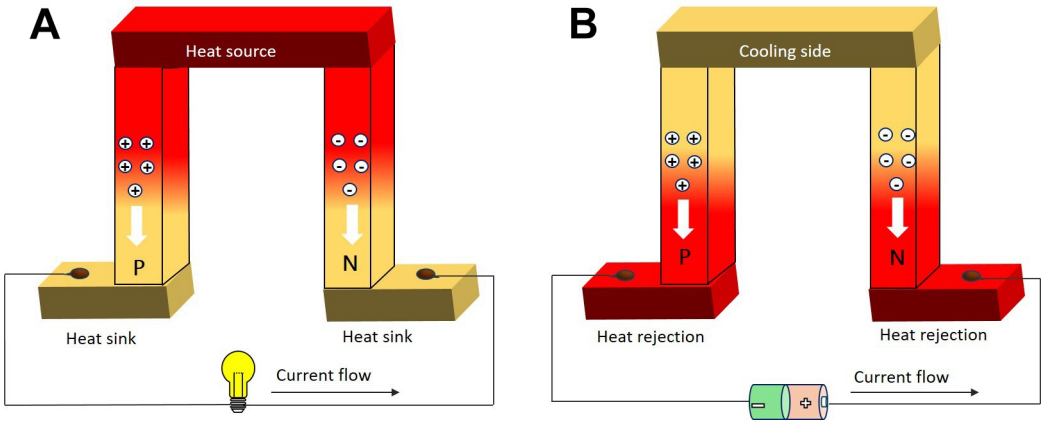

Figure 3. Schematic illustration of fundamental thermoelectric effects: (A) Seebeck effect, where a thermal gradient induces an electric potential, and (B) Peltier effect, showing heat exchange at junctions upon current flow.

of organic thermoelectric (OTE) materials is generally assessed based on the PF given by

$$PF = S^2\sigma \quad (2)$$

Therefore, *ZT* is frequently substituted with PF for assessing the TE performance of organic polymer materials and their corresponding composites, owing to their low thermal conductivity.

STATUS OF THERMOELECTRIC MATERIALS

P-type thermoelectric polymers

Conventional p-type TE polymers

The TE performance of various p-type conventional CP including PANI[67], PPy[68], polythiophene (PTH)[69], poly(3,4-ethylenedioxythiophene): poly(styrenesulfonate) (PEDOT:PSS)[70-73], polyacetylene (PA)[74,75], polycarbazoles (PC)[76], and their derivatives have been investigated, with their performance metrics summarized in Table 1[20,68,70,76-87]. Generally, the intrinsic conductivities of these CPs range from 10^{-16} to 10^{-5} S cm^{-1}, while their k are typically between 0.11 and 0.4 W m^{-1} K^{-1}, which contributes positively to their *ZT* values[88]. Currently, PF for most polymer-based TE materials falls within the range of 10^{-6} μW m^{-1} K^{-2} to 10^{-10} μW m^{-1} K^{-2}, significantly lower than those of traditional inorganic TE materials[89-92]. Among all these conventional TE polymers, PEDOT:PSS is a well-researched p-type TE material notable for its ease of processing and stability when heavily doped. Despite its promise, excess PSS acts as an insulator, hindering charge carrier transport and limiting its TE performance, with σ ranging from 0.012 S cm^{-1} to 17 S cm^{-1} and PF values from 0.0016 μW m^{-1} K^{-2} to 0.9 μW m^{-1} K^{-2}[70]. Numerous studies have sought to enhance the electrical properties of PEDOT:PSS, employing methods such as the introduction of polar solvents such as dimethylsulfoxide (DMSO) to encourage phase segregation and improve σ. Various post-treatment techniques have also been developed to optimize the structure and performance of PEDOT:PSS, such as the use of ionic liquids, reducing agents, and sequential acid-base treatments[72,93,94].

Research efforts have led to significant improvements in TE performance of PEDOT:PSS. However, PEDOT derivatives remain promising; challenges such as hygroscopicity and insulating counterions have driven researchers to explore new p-type TE polymers that may exhibit superior charge-transport characteristics.

Diketopyrrolopyrrole based p-type TE polymers.

DPP has gained considerable attention due to its unique electronic properties and versatility in molecular design. Its strong electron-accepting features, combined with its high planarity and robust thermal stability, make it an ideal candidate for enhancing the performance of organic TE devices. Recent advancements in DPP-based materials have led to significant improvements in charge carrier mobility and thermoelectric efficiency, paving the way for innovative applications in organic electronics. Figure 4 displays the chemical structures of several DPP-based p-type D-A polymers and Table 2 summarizes their optimal doped TE performance.

In 2017, Jung *et al.* synthesized poly(diketopyrrolopyrrole-terthiophene) (PDPP3T) due to its excellent performance in field of OFET. The study compares the thermoelectric efficiency of the DPP semiconductor PDPP3T against conventional thermoelectric polymer poly(3-hexylthiophene) (P3HT). By finely doping with $FeCl_3$, PDPP-3T has higher than 200 μW m^{-1} K^{-2} PFs and peaks at 276 μW m^{-1} K^{-2}, which is far more than the 56 μW m^{-1} K^{-2} PF of P3HT. High mobility PDPP3T increases σ without having a high dopant volume. It can be highly transparent due to a low band gap in electronic devices. In general, PDPP3T has all the attributes of high mobility, low band gap and well-controlled doping, to be a new gold standard for thermoelectric semiconducting polymers[95]. Besides, Liang *et al.* investigated the doping effects on PDPP-4T; they employed the strong oxidative compound Mo(tfd-CO_2Me)$_3$ and compared its performance to that of $FeCl_3$. While Mo(tfd-CO_2Me)$_3$ exhibits greater oxidative strength, its larger size as a dopant leads to significant disorder within the crystalline portion of the PDPP-4T. This disruption negatively affects the charge transport pathways, causing poor σ. Consequently, Mo(tfd-CO_2Me)$_3$-doped PDPP-4T exhibited σ of approximately 0.3 S cm^{-1} and a PF of around 15 μW m^{-1} K^{-2}. In contrast, $FeCl_3$-doped PDPP-4T demonstrated much higher conductivity of about 10 S cm^{-1} and a PF of approximately 23.5 μW m^{-1} K^{-2}. This comparison highlights that despite the potential advantages of using more powerful oxidants such as Mo(tfd-CO_2Me)$_3$, the effective doping of CP such as PDPP-4T may rely heavily on the dopant's size and its ability to maintain the integrity of the polymer's crystalline structure, which is critical for facilitating

Table 1. Thermoelectric performance of conventional polymers

Sr. no.	Polymer	k W $m^{-1}K^{-1}$	[S cm^{-1}]	S [μV K^{-1}]	ZT_{max}	Ref.
1	PEDOT:PSS	0.34	0.06-945	8-888	1×10^{-2} at 300 K	[70,77,78]
2	PEDOT:Tos	0.37	6×10^{-2}-300	40-700	0.25 at RT	[20]
3	PANI	0.02-0.542	10^{-7}-320	-16-225	1.1×10^{-2} at 423K	[79-82]
4	PPy	0.2	6×10^{-2}-300	-1-40	3×10^{-2} at 423K	[68,83]
5	PTH	0.028-0.17	10^{-2}-10^{-3}	10-100	2.9×10^{-2} at 250 K	[84-86]
6	PC	0.34	4×10^{-5}-5×10^{-2}	4.9-600		[76,87]

PEDOT:PSS: Poly(3,4-ethylenedioxythiophene): poly(styrenesulfonate); PANI: PPy: polypyrrole; PTH: polythiophene; PC: polycarbazoles; PEDOT:Tos: poly(3,4-ethylenedioxythiophene): tosylate.

efficient charge transport[96].

In 2020, Liu *et al.* investigated incorporation thiophene unit in the structure of PDPP-4T and synthesized PDPPT-5T and further modified the structure by replacing one thiophene unit with EDOT yielding PDPPT-4T-EDOT. From the study, it has been ascertained that PDPP-4T-EDOT can attain comparatively higher values of the Highest Occupied Molecular Orbital (HOMO), which facilitates efficient p-doping. Theoretical calculations indicate that PDPP-4T-EDOT exhibits slightly improved coplanarity compared to PDPP-5T to enhance charge carrier transport. Both polymers exhibit an increase in σ with an initial increase in dopant concentration, but the σ decreases at higher concentrations and with it, the S also reduces. The PF that the best results obtained by PDPP-4T-EDOT at a doping concentration of 0.5 mM was 298.2 μW m^{-1} K^{-2}, which is significantly superior to the value of 11.1 μW m^{-1} K^{-2} for PDPP-5T at 6 mM, as PDPP-4T-EDOT gets easily doped due to its higher HOMO energy level. This work serves as proof that engineering the energy levels by the incorporation of EDOT is beneficial for the developing high-performance p-type thermoelectric polymers[97].

Similarly earlier on, selenophene substitution was demonstrated to be an effective approach for improving intermolecular interactions and achieving high charge carrier mobility[98-100]. Ding *et al.* designed and synthesized selenium-substituted DPP-based polymer for TE devices. They modified the PDPP-3T structure by introducing a branched side chain on one side and a linear alkyl chain on the other end of each DPP unit, resulting in PDPPS-12. The structure was further modified by replacing one sulfur atom with selenium to obtain PDPPSe-12. The incorporation of selenium leads to strong intermolecular interactions and ordered molecular packing. PDPPSe-12, a DPP-selenophene copolymer, displayed impressive hole mobility, approaching 7 cm^2 V^{-1} s^{-1}. Its maximal σ, when doped with $FeCl_3$, is nearly 997 S cm^{-1}, over three times that of the doped PDPPS-12. Stronger intermolecular interactions occur within PDPPSe-12 because of larger atomic radius of selenium compared to that of sulfur. As a result, PDPPSe-12's molecular arrangement remains mainly unaltered by doping, although PDPPS-12's structure becomes less organized under similar doping conditions. Atomic force microscopy (AFM) analysis revealed that $FeCl_3$ doping profoundly altered the morphology of PDPPS-12 by demolishing its fiber-like polycrystalline microstructure and reducing the surface roughness. On the other hand, PDPPSe-12 retained its fiber-like intercalating network and exhibited negligible morphological alteration upon doping. This suggests better dopant accommodation in PDPPSe-12 with maintenance of its microstructure and facilitation of stable charge transport.

Notably, at low doping levels, PDPPSe-12 exhibits a remarkable hole mobility of around 1.9 cm^2 V^{-1} s^{-1}, leading to a maximum PF of 364 μW m^{-1} K^{-2}, which contributes to a ZT value of 0.25-marking a record for CP. This work provides insights into the structure-property relationship of doped OSc and indicates a pathway for the rational design of high-performance OTE materials[101].

Table 2. Summary of thermoelectric performances on DPP-based p-type thermoelectric D-A polymers at the optimized doping condition

Sr. no.	Polymer	Dopants	σ [S cm^{-1}]	*S* [μV K^{-1}]	PF [μW m^{-1} K^{-2}]	Ref.
1	PDPP-3T	FeCl3	55	226	276	[95]
2	PDPP-4T	FeCl3	10	150	23.5	[96]
		$Mo(tfd\text{-}CO_2Me)_3$	0.3	220	15	
3	PDPP-5T	FeCl3	120	42.2	11.1	[97]
4	PDPP-4T-EDOT	FeCl3	272	174.2	298.2	
5	PDPPS-12T	FeCl3	318	80	178	[101]
6	PDPPSe-12T	FeCl3	997	62	364	
7	EHT6-20DPP	FeCl3	93.3	78	56.7	[102]
8	PDPP-TT	FeCl3	45	92	38	[103]
9	$PDPP\text{-}g_32T_{0.3}$	FeCl3	360	56	110	
10	PDPPS-5	FeCl3	96.0	52.4	26.4	[104]
11	PDTP-DPP	FeCl3	58	39.8	10.8	[105]
12	PCZ-DPP	FeCl3	2.5	75	1.8	
13	C6-ICPDPP	FeCl3	0.204	254	1.32	[106]
14	DPP-MeDTP	FeCl3	92.8	80.9	60.7	[107]
		F4TCNQ	14.6	242	85.2	
15	PCD-1	F4TCNQ	$0.64_{(Mixing)}$ $0.80_{(Spin\ coating)}$	$307_{(Mixing)}$ $334_{(Spin\ coating)}$	$6.1_{(Mixing)}$ $9.0_{(Spin\ coating)}$	[108]
16	PCD-2	F4TCNQ	$3.1_{(Mixing)}$ $1.3_{(Spin\ coating)}$	$266_{(Mixing)}$ $321_{(Spin\ coating)}$	$21.8_{(Mixing)}$ $13.6_{(Spin\ coating)}$	
17	PCD-3	F4TCNQ	$0.02_{(Mixing)}$ $0.84_{(Spin\ coating)}$	$464_{(Mixing)}$ $431_{(Spin\ coating)}$	$0.47_{(Mixing)}$ $15.6_{(Spin\ coating)}$	
18	P(BDTTT-DPP)	FeCl3	1.8	193.7	6.5	[110]
19	P(BDT-DPP)	FeCl3	0.10	161	0.26	
20	P10	FeCl3	0.2	360	3.1	[111]
21	P12	FeCl3	8	124	12.3	
22	P01	FeCl3	8.8	103	9.5	
23	P29DPP-BT	FeCl3	298	72	158	[112]
24	P29DPP-BTOM	FeCl3	242.4	111	195	
		F4TCNQ	89	122	132	
25	CN1	FeCl3	56	122	79	[113]
26	CN3	FeCl3	78	95	65	
27	CN5	FeCl3	66	96	59	
28	CN7	FeCl3	15	155	34	
29	CN9	FeCl3	13	58	10	
30	PDPP	FeCl3	152	33	17	[119]
31	DITT30	FeCl3	38	57	12.5	
32	DITT80	FeCl3	2.6	87.5	2.01	
33	DITT100	FeCl3	1.6	138	3.0	

DPP: Diketopyrrolopyrrole.

In 2021 Kim *et al.* synthesized a novel DPP-based conjugated polymer, EHT6-20DPP, containing eight thiophene units in its repeat unit structure. The incorporation of multiple thiophene groups leads to increased doping efficiency with the p-type dopant $FeCl_3$ and thus improves thermoelectric properties. EHT6-20DPP achieves an σ of 93.28 S cm^{-1} along with a PF of 56.73 μW m^{-1} K^{-2}, performing considerably better than the reference DPP polymer, PDPP3T, with three thiophene units. There is a close similarity in saturation field-effect mobilities in their undoped states for both polymers, but the conductivity of

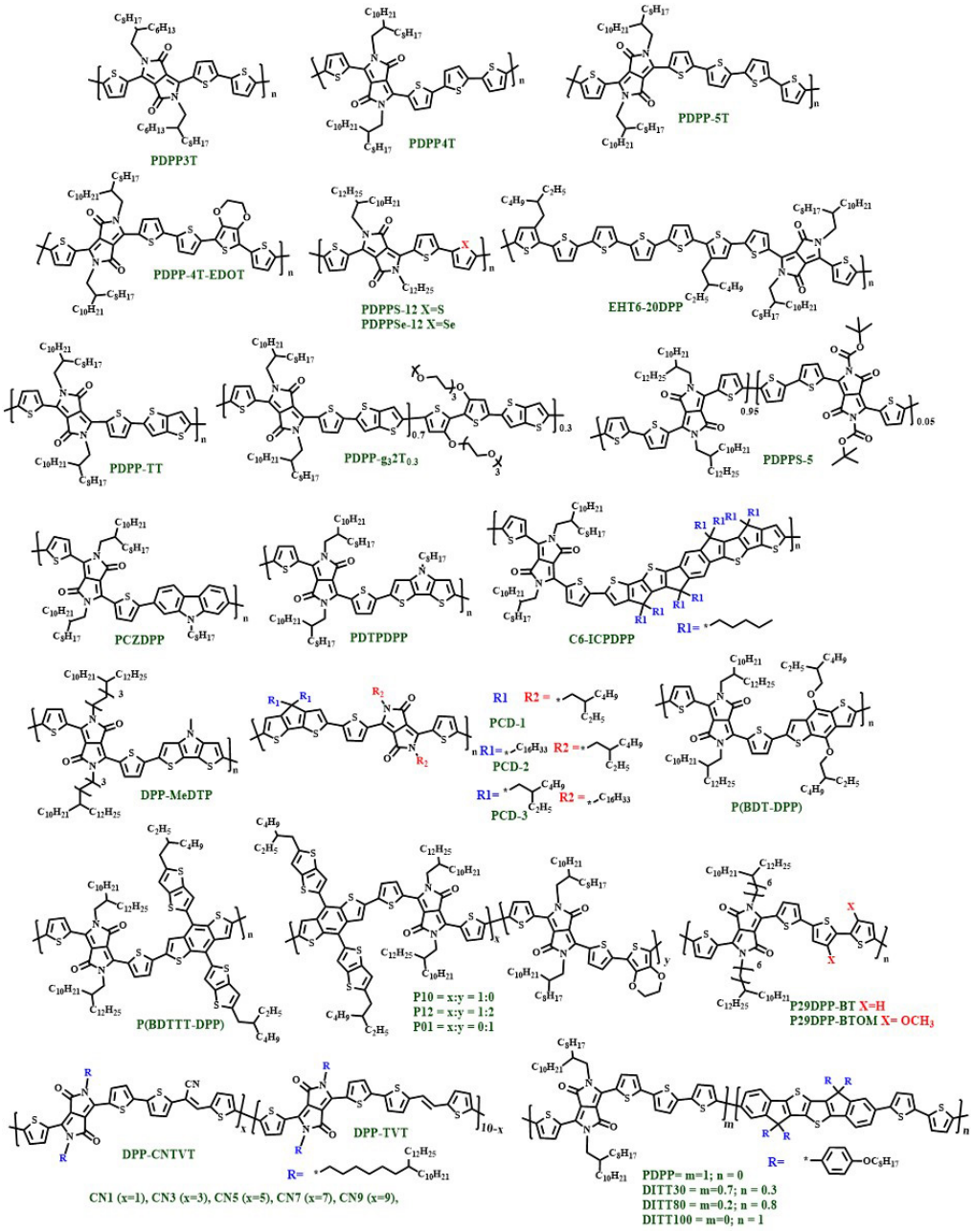

Figure 4. Chemical structure of a DPP-based p-type donor-acceptor polymer used in organic thermoelectrics. DPP:

EHT6-20DPP shows a remarkable increase against doping. The enhancement in TE performance is due to effective p-doping, and its good transport mechanism[102].

Side-chain engineering has become a key method for developing DPP-based D-A TE polymers, enabling the optimization of dopant miscibility and tuning of physical parameters. One example is the copolymerization and combination of thienothiophene (TT) with oligo ethylene glycol (OEG) bithiophene functionalized with side-chain on donating framework. In this study, the design of new random copolymers incorporating planar DPP as an acceptor unit alongside TT and OEG functionalized bithiophene as donor units. Key design principles include promoting strong interchain donor-acceptor interactions through the inclusion of

DPP-TT, which facilitates efficient charge transport via close packing and crystalline microstructures. The introduction of g32T-TT raises the HOMO level, improving charge transfer upon doping. Additionally, the dual incorporation of long alkyl chains and OEG side chains improves solubility and stabilizes dopants while fine-tuning the morphology of the films. Notably, the copolymer PDPP-$g_32T_{0.3}$ achieves an impressive σ of 360 S cm^{-1}, S of 56 μV K^{-1}, and PF of 110 μW m^{-1} K^{-2}, significantly outperforming its counterparts PDPP-TT having PF 38 μW m^{-1} K^{-2}. The enhanced doping efficiency, high carrier mobility exceeding 1 cm^2 V^{-1} s^{-1}, and improved crystallinity marked by strong π-π stacking contribute to the exceptional TE performance of these random copolymers, highlighting their potential for flexible electronic applications[103]. Mao *et al.* come up with a novel strategy that involves improvement in the crystallinity of the D-A polymer using the incorporation of tert-butoxycarbonyl (t-Boc) groups as thermos-cleavable side chains in p-type donor-acceptor DPP-based copolymers (PDPPS-X) for enhancement in the TE performance. The bulky and branched t-Boc groups ensure the polymers maintain good solubility for effective solution processing, while their subsequent removal significantly improves intermolecular stacking, leading to enhanced charge mobility. Thermal treatment facilitates crystalline domain formation through hydrogen-bonded networks, crucial for conductivity improvements. Results showed that PDPPS-5, tailored with optimal thermocleavable side chains, achieved the highest PF of 26.4 μW m^{-1} K^{-2} and σ of 96.0 S cm^{-1} at room temperature. Thus, the strategic incorporation of thermo-cleavable side chains effectively enhances crystallinity, charge mobility, and ultimately, TE performance[104].

Zhong *et al.* come up with a strategic approach to enhance the TE performance of D-A polymers through donor engineering, specifically by substituting the dithieno[3,2-b:2',3'-d]pyrrole (DTP) moiety (PDTP-DPP) with a carbazole (CZ) unit (PCZ-DPP) while retaining the DPP acceptor. This modification results in significantly elevated HOMO levels and reduced energy gaps, facilitating more effective p-doping. Density functional theory (DFT) calculations indicate that PDTP-DPP exhibits expanded HOMO distributions and decreased structural disorder compared to PCZ-DPP, which lowers the Coulomb and charge transfer energy barriers at varying doping concentrations. Consequently, even though PCZ-DPP has a higher intrinsic hole mobility (0.01 cm^2 V^{-1} s^{-1}) than PDTP-DPP (0.005 cm^2 V^{-1} s^{-1}), the TE performance of PDTP-DPP is noticeably superior, achieving an optimal PF of 10.8 μW m^{-1} K^{-2}-fivefold greater than that of PCZ-DPP which has a PF of 1.8 μW m^{-1} K^{-2}. Additionally, at elevated temperatures (488K), PDTP-DPP demonstrates enhanced TE performance, with a PF exceeding 85.5 μW m^{-1} K^{-2}, attributed to its favorable molecular characteristics that support thermal-induced dedoping and thermally activated carrier hopping[105].

Lee *et al.* synthesized a new D-A conjugated polymer, C6-ICPDPP, to enhance TE performance by integrating electron-donating fused benzene, thiophene, and cyclopentadithiophene (CDT) units, with the electron-accepting DPP core in the polymer backbone. Through extended π-conjugation, this novel structural design promoted efficient charge transfer by achieving outstanding planarity. Using $FeCl_3$ only p-type dopants, C6-ICPDPP demonstrated both p-type and n-type thermoelectric activity, likely due to the bulk of charge carriers from positive to negative as the concentration of $FeCl_3$ doping increases. The impact of solvent type [chlorobenzene (CB) and chloroform] on film morphology, doping efficiency, and oxidation degree was also systematically investigated. Films processed from CB, a solvent with a higher boiling point, showed enhanced dopant diffusion and a greater degree of oxidation, contributing to improved TE performance. Two optimized PFs and σ were obtained for p-type: 1.32 μW m^{-1} K^{-2} and 0.204 S cm^{-1} and n-type: 0.410 μW m^{-1} K^{-2} and 0.0664 S cm^{-1}. The extended planar backbones in D-A CP appears great potential to optimize thermoelectric properties, with the prospects for p-type and n-type behavior using a single dopant, whereby the effect of solvent and film structure on device performances is realized[106]. Furthermore, DPP-MeDTP polymer has demonstrated improved thermoelectric properties through the

introduction of extended branched 7-decylnonadecyl side chains on DTP donor unit into a DPP-based conjugated polymer which was synthesized by Lee *et al.*[107]. DPP-MeDTP polymer, exhibited high TE performance with high σ due to high planarity and crystallinity, leading to a PF as high as 85.2 μW m^{-1} K^{-2} with F4TCNQ doping that turned out to be a multiple of other polymers in the trial. $FeCl_3$-doped polymer showed PF of 60.7 μW m^{-1} K^{-2}. Although most other dopants can show higher PF with $FeCl_3$ doping due to higher doping levels, the F4TCNQ-DPP-MeDTP doped polymer had a high S of 242 μV K^{-1}, thus giving it a superior PF. Suh *et al.* came up with a new approach. They incorporated fused cyclopenta[2,1-b:3,4-b']dithiophene (CDT) moieties in the donor part of DPP-based D-A CP, resulting in three new polymers, namely, PCD-1 with branched side chains on the CDT and DPP units; PCD-2 with linear side chains on the CDT unit; and PCD-3 with linear side chains on the DPP unit[108]. The highly aggregated polymers, PCD-1 and PCD-2, primarily formed ion pairs with the F4TCNQ, thus facilitating further aggregation in the thin film and as a result gave rise to high σ of 0.64 and 3.1 S cm^{-1}, respectively. Among these, PCD-2 achieved the highest PF of 21.8 μW m^{-1} K^{-2}. In contrast, PCD-3, which exhibited less aggregation, showed much lower conductivity (0.02 S cm^{-1}) and a PF of 0.47 μW m^{-1} K^{-2}, attributed to its lower doping efficiency and the formation of Lewis complexes with the dopant. Using the sequential doping technique, the polymer chains were fully aggregated in the solution, regardless of the presence of dopants. As a result, the PF values of PCD-1, PCD-2, and PCD-3 became much closer to each other, with values of 9.0, 13.6, and 15.6 μW m^{-1} K^{-2}, respectively.

In 2021, Li *et al.* chose a benzodithiophene (BDT) donor building block whose fused-ring structure causes high planarity and a narrow band gap, and it possesses excellent electron-donating properties[109]. Furthermore, to enhance backbone planarity, the TT unit can also be incorporated into the side chain to form the BDTTT donor unit and combined it with DPP to generate a two-dimensional (2D) P(BDTTT-DPP) CP[110]. The resultant 2D polymer P(BDTTT-DPP) possesses a better molecular stacking ability than the one-dimensional (1D) P(BDT-DPP) with branched alkoxy chain synthesized for TE performance comparison. When both compounds were doped with FeCl3, P(BDTTT-DPP) exhibited a remarkably higher σ of 1.83 S cm^{-1}, which was 20 times higher than that of the corresponding P(BDT-DPP) and produced a PF of 6.50 μW m^{-1} K^{-2}, 26 times that of P(BDT-DPP). As the temperature ranged, PF increased, reaching a maximum value of 10.50 μW m^{-1} K^{-2} at 350 K. The significant augmentation in TE performance was attributed to the enhanced doping level and better π-π stacking in P(BDTTT-DPP), hence suggesting that incorporating 2D conjugated units into D-A polymers could substantially enhance thermoelectric properties.

At the same time, another innovative approach was made by Cao *et al.* to enhance the TE performance by using D-A copolymers with 1D EDOT framework with 2D BDTTT units, being randomly copolymerized to combine the high-Seebeck-coefficient of BDTTT with the strong-doping tendency of EDOT[111]. The copolymer P12 demonstrates a superior PF of 12.3 μW m^{-1} K^{-2}, which is significantly higher than P10 (3.1 μW m^{-1} K^{-2}), with only BDTTT as the donor part, and P01 with PF of 9.5 μW m^{-1} K^{-2}, which has only EDOT as the donor unit.

Significant efforts have been made by Lee *et al.* to enhance the TE performance. Recently, they have designed and synthesized methoxy-functionalization donor-acceptor conjugated polymer based on DPP and bithiophene units and compared the performance between the methoxy-functionalized polymer, P29DPP-BTOM and its unfunctionalized counterpart, P29DPP-BT. The introduction of methoxy group increased lamellar stacking distance which enhanced the dopant's diffusion and consequently its doping efficiency, notably for the bigger dopants. Hence, the methoxy-functionalized polymer, P29DPP-BTOM, had increased carrier concentration and mobility when compared with P29DPP-BT. In the case of the $FeCl_3$

dopant, the resulting TE performance based on P29DPP-BTOM was impressive, with a maximum σ reaching 242.4 S cm^{-1} and a charge carrier mobility of 0.18 cm^2 V^{-1} s^{-1} when compared to 298 S cm^{-1} and 2.44 cm^2 V^{-1} s^{-1} in the case of P29DPP-BT. Further comparison reveals that P29DPP-BTOM exhibited an even larger S, thereby providing a PF of 195.1 μW m^{-1} K^{-2} and that of a doped P29DPP-BT being only 158.3 μW m^{-1} K^{-2}. Additionally, doping with F4TCNQ only worked for P29DPP-BTOM, although the maximum σ was lower (88.9 S cm^{-1}), thereby highlighting the stronger doping efficiency of $FeCl_3$[112]. Both F4TCNQ and $FeCl_3$ doped P29DPP-BTOM films exhibit highly similar crystalline structures, which indicates that dopant size and structure did not affect film microstructure. This is due to the fact that the extensive lamellar spacing and sufficient free volume between alkyl side chains allow for successful accommodation of the dopant. Thus, lower oxidation strength in the F4TCNQ-doped film is the reason for its lower conductivity, not differences in crystallinity. Furthermore, the impact of electronic structures in D-A conjugated polymers on their TE properties was systematically investigated by synthesizing a series of random D-A copolymers with similar crystalline structures. These copolymers were designed by varying the ratio of two building blocks: the donor DPP-TVT and the acceptor DPP-CNTVT, with DPP-CNTVT incorporating an electron-withdrawing cyano group on its vinylene moiety[113]. The doped copolymers were then studied for their doping behavior and thermoelectric properties, with p-type doping using $FeCl_3$ and n-type doping using 4-(2,3-dihydro-1,3-dimethyl-1H-benzimidazol-2-yl)-N,N-dimethylbenzenamine (N-DMBI). The incorporation of DPP-TVT raised the HOMO levels as well as the doping efficiency with $FeCl_3$. The PF and the μ were found to be maximum with the copolymer with the lowest amount of DPP-CNTVT (CN1), which gave a maximum PF value of 79.8 μW m^{-1} K^{-2}. The decrease in PF with higher DPP-CNTVT content was attributed to polaron localization caused by the acceptor's electronic structure. Single polymer with both thermoelectric properties and stretchability for self-powered wearable electronics is challenging. One straightforward way to develop intrinsically stretchable OTE (IS-OTE) polymers is through the incorporation of aliphatic breakers into the polymer's backbone[114-116]. However, this usually decreases charge carrier mobility. An alternative would be to increase amorphous regions in the polymer by incorporating fused-ring conjugated breakers, which might benefit the dissipation of stress during mechanical deformation[117,118]. By applying the above strategy, Tseng *et al.* synthesized novel IS-OTE polymers by introducing a fused DITT unit into the polymer backbone. Nevertheless, the rigid coplanar structure of DITT ensures efficient charge transport across amorphous domains of the polymer. Varying the amounts of DITT in its copolymer with respect to quantity of DPP will balance the amorphous and crystalline regions and render stretchable polymers such as these with enhanced TE performance. The copolymer exhibited high PF of 12.5 μW m^{-1} K^{-2} achieved by DITT30, with an impressive crack onset strain of over 100%, maintaining 80% of its original PF after 200 stretch-release cycles. This work has shown the first case of an IS-OTE polymer capable of bright potential applications in the field of wearable electronics[119].

Diketopyrrolopyrrole-based n-type thermoelectric polymers

Even though significant amount of research has been carried out on p-type TE materials and dopants in recent decades, studies of their n-type counterparts have significantly lagged behind those of p-type materials due to a variety of intrinsic and extrinsic limitations. One of the fundamental issues is the relatively low electron affinity (EA) of most conjugated polymers, which makes efficient and stable n-type doping difficult[120]. Additionally, n-type dopants tend to be more air-sensitive, chemically labile, or have harsh doping conditions such as high temperature or vacuum treatment that prevent practical use and scalability[121-123]. Furthermore, poor miscibility and limited dopant-polymer backbone compatibility often result in inhomogeneous doping, phase segregation, or inefficient charge transfer, resulting in reduced conductivity[124]. Some p-type materials have reached σ of over 1000 S cm^{-1}[20]. With the increasing demand for high-performance OTE materials, the development of n-type CPs has been one of the major focuses of research; most n-type materials have low σ, and only a few of them have reached σ values above 1 S cm^{-1}

after doping[22]. As a result, there has been growing interest in n-type materials and dopants, leading to significant advancements in the development of new n-type TE materials. The designed strategy for good n-type TE materials requires careful tuning of their lowest unoccupied molecular orbital (LUMO) energy levels. A reduced LUMO facilitates thermodynamically favorable electron transfer from the dopant to the polymer and thereby enhances n-doping efficiency[125,126] and ambient stability because they resist quenching by environmental oxygen, water, or trap states[127,128]. The electronic nature of the polymer backbone also plays a very significant role in establishing the extent of polaron or bipolaron delocalization with doping[129]. A-A type backbones tend to have more charge delocalization than D-A systems[130]. Moreover, good mixing allows the dopant molecules to be well dispersed in the polymer matrix without aggregating and ensures doping effectiveness without interfering with charge mobility[131]. Close and well-ordered packing of polymer backbones is crucial for the formation of an ideal morphology when doped. In such structures, molecular dopants tend to localize within the amorphous regions, where efficient electron transfer is possible, and the crystalline domains remain comparatively unperturbed for efficient charge transport[101,132]. Additionally, face-on and edge-on mixed stacking arrangements have been demonstrated to trade off doping efficiency and charge transport via improved dopant accommodation[133,134]. Therefore, the solid-state packing and backbone alignment optimization is a critical approach to realize high σ and comprehensive TE performance in n-type CPs.

Currently, various kinds of n-type building blocks are used for the development of n-type OTE materials, such as naphthalene diimide (NDI)[135,136], perylene diimide (PDI)[130], benzodifurandione polyphenylenevinylene (BDOPV)[137,138], and bithiophene diimide (BTI)[139,140]. Among these, the most used electron-deficient building block for n-type OTE is NDI, and its representative compound would be N2200[141]. The compound has an σ of about 10^{-3} S cm^{-1} and a PF of about 10^{-2} μW $m^{-1}K^{-2}$[135]. In other words, it is of the utmost importance for the production of n-type OTE materials in order to develop new electron-deficient blocks. DPP has also attracted much attention as versatile unit for n-type semiconducting polymer due to its very strong electron-accepting character, planarity, and ease of synthesis for two decades[29,50,53,142]. However, the presence of the electron-rich thiophene side groups in DPP leads to high frontier molecular orbitals (FMOs) energy levels and consequently renders DPP-based copolymers to often display p-type or ambipolar transport properties, which severely limits their assessments as effective n-type materials in OTEs[143]. Connecting of two thiophene units with a central DPP core generates the 1,4-diketopyrrole[3,4-c]pyrrole dithiophene (DBT), which exhibits ambipolar nature and demonstrates exceptionally high hole mobility 10 cm^2 V^{-1} s^{-1}[144]. To further improve the electron mobility (μ_e) of DPP-based polymers, Sun *et al.* synthesized DBPy by substituting the electron-rich thiophene by the more electron-deficient pyridine. The copolymer of DBPy and bithiophene (PDBPyBT) exhibited significantly improved μ_e of 6.30 cm^2 V^{-1} s^{-1}. Such enhancements are crucial for the optimization of the performance of n-type materials utilized in TE devices[144]. The potential application of DPP-based polymers for n-type OTE devices, first developed by Yang *et al.,* was demonstrated in 2018. They synthesized two polymers, namely Poly[2,5-bis(2-octyldodecyl)-3,6-di(pyridin-2-yl)-pyrrolo[3,4-c]pyrrole-1,4(2H,5H)-dionealt-(E)-2,2'-(ethene-1,2-diylbis(3,4-difluorothiophene-5,2-diyl)) (PDPF) and Poly[2,5-bis(2-octyldodecyl)-3,6-di(pyridin-2-yl)-pyrrolo[3,4-c]pyrrole-1,4(2H,5H)-dionealt-(E)-2,2'-(ethene-1,2-diylbis(thiophene-5,2-diyl))] (PDPH), with and without fluorine substituents possessing electron-withdrawing capability respectively[133]. Figure 5 displays the chemical structures of several DPP-based n-type D-A polymers and Table 3 summarizes their optimal doped TE performance. The lower energy of LUMO (E_{LUMO}) of PDPF, which contained fluorine, was measured at -4.11 eV, while that of PDPH was close to -3.93 eV. This means that PDPF has more affinity to electrons than PDPH, an important factor for n-type performance in thermoelectrics. PDPH shows nonuniform doping, with areas of the film exhibiting variable doping concentrations that may affect its overall performance. In contrast, PDPF has a more uniform distribution of dopants due to the structural binodal backbones, which is believed to allow multiple packing

Table 3. Summary of thermoelectric performances of DPP-based n-type thermoelectric polymers at the optimized doping condition

Sr. no.	Polymer	Dopants	σ [S cm^{-1}]	*S* [μV K^{-1}]	PF [μW m^{-1} K^{-2}]	Ref.
1	PDPH	N-DMBI	1.01×10^{-3}	-80	5.11×10^{-4}	[133]
2	PDPF	N-DMBI	1.3	-235	4.65	
3	P(TDPP-CT2)	N-DMBI	0.39	-580	9.3	[123]
4	P(PzDPP-CT2)	N-DMBI	8.4	-370	57.3	
5	P(PzDPP-2FT)	$CoCp_2$	129	-	-	[145]
6	PDCNBT-DPP	N-DMBI-H	11.78	-146	7.96	[146]
7	PDCNBSe-DPP	N-DMBI-H	12.36	-102	9.22	
8	PTz-5-DPP	N-DMBI	8.39	-338	106	[147]
9	P(DPP-CNPz)	N-DMBI	25.30	-131.9	41.4	[148]
10	P(DPP-DCNPz)	N-DMBI	33.94	-95.25	30.4	
11	ThDPP-CNBTz	N-DMBI	50.6	-145	126	[149]
12	pDSe	N-DMBI	5.9	-217.9	27.8	[150].
13	pDFSe	N-DMBI	62.6	-154.8	133.1	
14	PTh-DPP	N-DMBI	0.03	-403.7	0.5	[151]
15	PThTz-DPP	N-DMBI	0.68	-277.0	5.2	
16	PTz-DPP	N-DMBI	63.2	-133.0	111.8	

PDPH: Poly[2,5-bis(2-octyldodecyl)-3,6-di(pyridin-2-yl)-pyrrolo[3,4-c]pyrrole-1,4(2H,5H)-dionealt-(E)-2,2′-(ethene-1,2-diylbis(thiophene-5,2-diyl))]; PDPF: Poly[2,5-bis(2-octyldodecyl)-3,6-di(pyridin-2-yl)-pyrrolo[3,4-c]pyrrole-1,4(2H,5H)-dionealt-(E)-2,2′-(ethene-1,2-diylbis(3,4-difluorothiophene-5,2-diyl)).

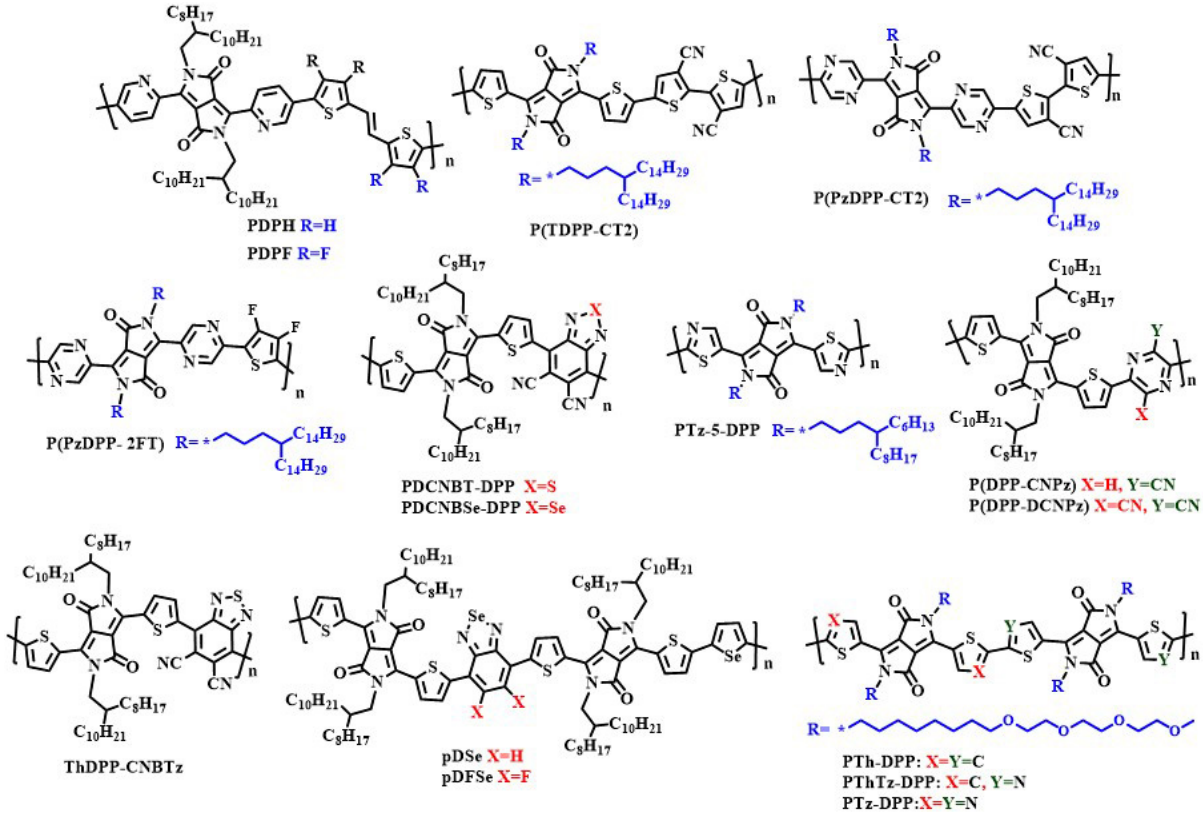

Figure 5. Chemical structure of a DPP-based n-type donor-acceptor polymer used in organic thermoelectrics. DPP:

orientations. This would imply more space where the dopants could reside, capable of ensuring more effective and even doping within the film. As a result of these structural advantages, PDPF demonstrated much higher σ and PF values compared to PDPH. The TE performance resulted in a maximum σ of 1.30 S cm^{-1} with a PF of 4.65 μW m^{-1} K^{-2} for PDPF. In contrast, the less effective doping profile allowed for only a σ of 1.01 × 10^{-4} S cm^{-1} with a PF of 5.11 × 10^{-4} μW m^{-1} K^{-2} for PDPH. Later, Yan *et al.* designed and synthesized a more electron-deficient structural backbone based on DPP, entitled PzDPP and its polymer P(PzDPP-CT2)[123]. The polymer was designed by substituting the bithiophene units in P(TDPP-CT2) with pyrazine moieties and copolymerizing it with a cyano-functionalized bithiophene as an electron-deficient moiety. The resultant polymer P(PzDPP-CT2) exhibited a much lower E_{LUMO} of -3.45 eV compared to -2.85 eV for dibenzothiophene and -3.06 eV for pyridine flanked-DPP (PyDPP). The introduction of the pyrazine unit gave rise to considerable intramolecular hydrogen bonding, which helped the polymers gain additional rigidity and planarity in their backbones. Such structural enhancements resulted in efficient charge transport along the chains, leading to 0.79 cm^2 V^{-1} s^{-1} electron mobility (μ_e) for P(PzDPP-CT2), which was significantly higher than the above-mentioned 0.32 cm^2 V^{-1} s^{-1} for P(TDPP-CT2). This enabled P(PzDPP-CT2) to achieve an excellent maximum σ of 8.4 S cm^{-1} and PF of 57.3 μW m^{-1} K^{-2}, marking the highest performance reported for DPP-based n-type TE materials. Furthermore, Yan *et al.* computationally designed a new pyrazine-based polymer, P(PzDPP-2FT), which features fluorine substitutions at the thiophene sites[145]. This novel structure benefits from the presence of intrachain noncovalent hydrogen bonding interactions between the DPP, pyrazine, and fluorine units. One of the many interesting features of P(PzDPP-2FT) is that it tolerates disorder caused by doping. In fact, the original paracrystalline structure was retained when up to 60% concentration was reached with N,N-dimethylbenzimidazole (N-DMBI). This remains a highly relevant characteristic as it enhances the stability and performance of the polymer through heavy doping conditions. Furthermore, when P(PzDPP-2FT) is doped with cobalt cyclopentadienyl ($CoCp_2$) , its σ significantly improves, achieving a value of 129 S cm^{-1}.

Recently, Wang *et al.* designed and synthesized new n-type TE polymers using novel approach that is development of A-A polymers designed strategy. This A-A strategy will help reduce intramolecular charge transfer (ICT) properties that influence the performance of semiconductors achieved with low FMOs. Therefore, they synthesized two A-A polymers based on this strategy namely, PDCNBT-DPP and PDCNBSe-DPP by integrating DPP with coplanar building block and cyano-functionalized benzothiadiazole (DCNBT) and benzoselenadiazole (DCNBSe) possessing high electron deficiency[146]. The synthesized polymers demonstrated very narrow bandgaps (~1.0 eV) and deep-lying LUMO energy levels of ~-3.90 eV, thus leading to n-type behavior within the OTE devices. The highest electrical conductivities, 11.78 and 12.36 S cm^{-1}, are displayed by PDCNBT-DPP and PDCNBSe-DPP following N-DMBI-H doping, respectively, contributing to high PFs of 7.96 and 9.22 μW m^{-1} K^{-2}. Relatively higher PF value obtained for the PDCNBSe-DPP than PDCNBT-DPP attributed to decrease in aromaticity and increase in quinodal nature of the acceptor unit when S was replaced with Se. Moreover, the PDCNBSe-DPP has low LUMO energy levels and high electron mobility than PDCNBT-DPP. These results highlight the fact that cyano-substituted benzoselenadiazole insertion into A-A-type polymers is a successful strategy for building high-performance n-type OTEs.

Shi *et al.* synthesized a new high-performance n-type homopolymer PTz-5-DPP, using firstly adopted C-H/C-H oxidative direct arylation polycondensation method using newly developed monomer 3,6-di(thiazol-5-yl)-diketopyrrolopyrrole (Tz-5-DPP). The polymer has demonstrated significant potential as an n-type OTE application. The PTz-5-DPP polymer displays both edge-on and face-on orientations in thin films with stable lamellar (22 Å) and π-π stacking (3.62 Å) distances prior to and after doping. After doping with N-DMBI, the crystallinity of the polymer was enhanced considerably as revealed through stronger and

sharper X-ray diffraction (XRD) peaks and larger lamellar coherence length from 68.9 Å (undoped) to 132.0 Å (50 wt% doped). From the AFM, they observed smooth surface in the undoped film (RMS 0.62 nm), while doped films exhibit granular morphology and a moderate roughness increase (up to 1.69 nm), indicating more ordered molecular packing without the formation of large aggregates. However, in general polymers with low crystallinity tend to have more disordered or flexible structures, which makes it easier for dopant molecules to mix in within the polymer matrix, but in the case of PTz-5-DPP, the polymer shows bimodal packing orientations. These mixed orientations naturally create transitional regions or interfaces between the two packing types. These regions can act as flexible zones that help to accommodate dopant molecules. Upon doping with N-DMBI, PTz-5-DPP achieved an impressive electron conductivity exceeding 8.38 S cm^{-1}. Moreover, it achieved a PF reaching up to 106.0 μW m^{-1} K^{-2}[147].

For thermoelectric applications, Tu *et al.* developed a novel class of structurally easy, low-cost, and easily available electron-deficient structural moiety for n-type polymers. They have come up with 3,6-dibromopyrazine-2-carbonitrile (CNPz) and 3,6-dibromopyrazine-2,5-dicarbonitrile (DCNPz), two cyano-functionalized pyrazine electron-deficient building blocks. Their great planarity is a major advantage for their use in n-type systems since the steric hindrance effect on the cyano-functionalized pyrazine building blocks has been theoretically studied. Two A-A type polymers, P(DPP-CNPz) and P(DPP-DCNPz), were synthesized from CNPz and DCNPz through incorporating them with the DPP unit[148]. The planar backbones and deep-lying LUMO levels of these polymers aid in the achievement of high n-type performance. The polymers exhibited unipolar electron mobilities of up to 1.85 cm^2 V^{-1} s^{-1} for P(DPP-DCNPz) and 0.85 cm^2 V^{-1} s^{-1} for P(DPP-CNPz). When doped with the molecular dopant N-DMBI, they revealed high PFs of 41.4 μWm^{-1} K^{-2} and 30.4 μWm^{-1} K^{-2}, along with outstanding electrical conductivities of 25.30 S cm^{-1} and 33.93 S cm^{-1}, respectively. The results point to CNPz and DCNPz as promising and cost-effective building blocks for the development of high-performance n-type polymer semiconductors.

Low crystallinity conjugated polymers have been considered to be potential candidates for OTEs, especially for flexible devices, since their disordered structure provides an efficient means of introducing dopants and retains high flexibility innately. Therefore, Gao *et al.* designed and synthesized two n-type conjugated polymers, ThDPP-BTz and ThDPP-CNBTz, low crystallinity polymers with dual acceptor backbone featuring a thiophene-flanked DPP and cyano-substituted benzothiadiazole[149]. Due to its low LUMO energy level of below -4.20 eV and low crystallinity, ThDPP-CNBTz achieved high doping efficiency and better polaron delocalization. After doping with *N*-DMBI, ThDPP-CNBTz realized high σ of 50.6 S cm^{-1} and a PF of 126.8 μW m^{-1} K^{-2} at the best, which is among the highest values reported for solution-processed n-doped polymers. A flexible OTE device also fabricated based on 20 mol% doped polymer; exhibits a maximum PF of 70 μW m^{-1} K^{-2} and excellent bending stability with almost no change in conductivity after 600 cycles. This finding provided a pathway for the development of high-performance n-type materials suitable for flexible OTE devices.

Recently, Shen *et al.* made a significant approach to enhance the performance of TE polymer by incorporation of noncovalently fused-ring strategy. They synthesized pDFSe conjugated polymer using unique acceptor-triad structure containing DPP and difluorobenzoselenadiazole with noncovalently fused-ring design, which improves the backbone rigidity[150]. Additionally, an axisymmetric thiophene-selenophene-thiophene donor was also incorporated in order to facilitate development of nearly amorphous microstructures, promoting effective intrachain charge-carrier mobility. The research confirms that pDFSe is of a close-to-amorphous nature, as supported by XRD and AFM results. XRD reveals a shorter crystalline correlation length (CCL) of 26.4 Å (~7 layers of π-stacking) for pDFSe compared to 36.3 Å (~10 layers) for more crystalline pDSe. In addition, the paracrystalline disorder parameter (g) of pDFSe is

around 21%, exceeding the 19% threshold widely used to describe amorphous polymers, whereas pDSe shows a lower g value of 17%, indicating some extent of minor semicrystallinity. Further, AFM also supports these findings, with pDFSe showing smooth and featureless morphology and low RMS roughness of 0.37 nm, compared to the more textured crystalline domains and higher roughness of 1.56 nm in pDSe. The amorphous nature of pDFSe allows for greater miscibility of dopants and easier accommodation of dopant ions, which translates to enhanced doping efficiency and potential for enhanced TE performance. As a result, n-type TE based on pDFSe exhibits excellent electron mobility of 6.15 $cm^2 V^{-1} s^{-1}$, significantly higher than 0.77 $cm^2 V^{-1} s^{-1}$ measured for the control polymer pDSe (without noncovalently fused-ring structure). After n-doping, pDFSe shows exceptional conductivity of 62.6 S cm^{-1} with a maximum PF of 133.1 μW $m^{-1} K^{-2}$, observed due to deeper LUMO better electron mobility and improved doping efficiency. The obtained result is among the highest for solution-processed n-type polymers. Very recent, Ma *et al.* designed and investigated a series of new n-type DPP-based conjugated polymers to study the influence of sp^2-nitrogen (N) introduction into the density of states (DOS) and the thermoelectric properties. Three polymers, PTh-DPP, PThTz-DPP, and PTz-DPP, with increasing numbers of sp^2-N atoms within the repeating unit by polymerizing thiophene-DPP and 3,6-di(thiazole-5-yl)-DPP-functionalized monomers. These structural modifications were coupled with the use of amphipathic side chains, which improved solubility and facilitated favorable morphology for TE devices[151]. Upon increase in the sp^2-N content, the deepening of the energy levels was observed.. The increased DOS facilitated better doping by offering greater electronic states accessible and promoting polaron formation as evidenced by greater ultraviolet-visible-near infrared (UV-vis-NIR) polaron absorption and higher spin densities in electron paramagnetic resonance (EPR) measurements. PTz-DPP, with the maximum sp^2-N content, showed the best doping response and showed least structural perturbation upon doping, retaining molecular order and intimate π-π stacking (0.36 nm), which are essential for efficient charge transport. After doping with N-DMBI, PTz-DPP possessed a superior σ of 63.8 S cm^{-1} and a PF of 111.8 μW $m^{-1} K^{-2}$, which enabled it to possess a ZT of 0.46, placing it among the highest-performing n-type organic TE materials. The high TE performance of PTz-DPP was not only a result of improved doping efficiency but also a result of a change in the mechanism of charge transport from hopping (seen in PTh-DPP) to more coherent or band-like transport in PTz-DPP, as determined by Hall-effect measurements and temperature-dependent transport investigations. Moreover, the increased site density near the Fermi level led to shorter charge hopping distances and increased carrier mobility. This work highlights the key significance of molecular design specifically the strategic use of electron-deficient, nitrogen-rich heterocycles in managing the electronic structure and optimizing charge transport channels in n-type organic TE materials.

MOLECULAR DOPING OF THERMOELECTRIC POLYMERS

Doping is an effective approach to optimize the performance of CP thin films, mainly for thermoelectric application. With the presence of dopants, there is considerable enhancement in charge carrier concentration within the polymer matrix, leading to an improvement in the σ, a key component in realizing high thermoelectric efficiency. Chemical doping and electrochemical doping are the two primary techniques employed to dope CP thin films. Chemical doping is typically accomplished by introducing small molecular oxidizing or reducing agents into the CP matrix. The dopants interact with the polymer chains through charge transfer mechanisms. Good alignment in the energy levels enables the energy exchange to add or extract electrons, thus altering the electrical properties of the CP. Conversely, electrochemical doping is performed by casting the CP film on a conductive substrate, which is then immersed in an electrolyte solution. These two methods represent controllable and effective ways to modulate the electrical properties of CP thin films, which is important for their applications in high-performance TE devices.

Doping mechanism and method

The enhancement of σ in CPs is highly dependent on the doping strategy employed. Redox doping and acid/base doping are the two main doping mechanisms that have been commonly recognized as shown in Figure 6A. Electron transfer between the CP and a dopant species governs the redox doping process and in case of acid/base doping the CP interacts with acidic or basic species that can donate or accept protons (H^+) or hydride ions (H^-). Depending on the direction of charge movement, this electron exchange may result in either n-type or p-type doping. In particular, n-type doping takes place when electrons transport from the dopant's HOMO to the polymer's LUMO, whereas p-type doping happens when electrons move from HOMO of CP to LUMO of the dopant. The efficiency of this doping process is critically influenced by the relative alignment of the energy levels between the dopant and the polymer.

The selection of an appropriate dopant is one of the most important factors in optimizing the TE properties of CPs because it directly influences critical parameters such as σ, S, and overall PF. For effective p-type doping, the EA of the dopant must be greater than the ionization energy (IE) of the polymer ($EA_{dopant} > IE_{CP}$) for efficient charge transfer through the integer charge transfer (ICT) mechanism. Similarly, n-type doping requires dopants with ionization energies lower than the EA of the polymer ($EA_{CP} > IE_{dopant}$). This energy level compatibility not only enables efficient doping but also prevents the formation of trap states that would hinder charge mobility.

The method by which dopants are introduced into TE polymers significantly influences doping efficiency, morphology, and the resulting σ[152,153]. Among the commonly employed methods, the mixing doping and sequential doping methods are common techniques as shown in Figure 6B, in the mixing doping the dopant and CP are individually dissolved in suitable solvents, then mixed together in specific ratios to produce a homogeneous mixture. This one-step, simple process enables easy control of the doping level by simply adjusting the concentration of the dopant. At higher doping concentration of the dopant, dopant molecules form aggregates, inducing phase separation and disturbing the polymer microstructure. Such aggregation can disturb the packing of polymer chains, reduce film crystallinity, and form trap states that eventually hinder the mobility of charge carriers[154]. Apart from that, miscibility of the dopant with the polymer and dopant solubility in the chosen solvent system are major concerns to ensure a homogeneous doping effect. For instance, the low solubility of high-electron-affinity dopants such as F4TCNQ in the majority of organic solvents can restrict their applicability for the mixing approach. To address the limitations associated with mixing doping, sequential doping methods have been developed. The sequential doping method has several advantages over the mixing doping method[155,156]. In this method, the CP film is first cast and dried, then a solution of dopant is deposited on top of it. In spin-coating, a minute quantity of the dopant solution dissolved in a semi-orthogonal solvent that swells but doesn't dissolve the polymer is dispensed on the polymer surface and left to interact for a measured period of time. It is then spun rapidly to remove excess solution, giving a controlled and homogeneous doping layer. This method minimizes disruption of the native polymer morphology and helps preserve the chain packing and order, even at higher doping levels. The spin-coating process enables accurate control over the doping level by adjusting key parameters such as dopant concentration and contact time, resulting in enhanced electrical properties without compromising film integrity. Overall, mixing and spin-coating-based SQD both have advantages and challenges, and their selection should be guided by factors that include polymer-dopant compatibility, doping precision needed, and process scalability.

p-type dopants

To improve the TE performance of CPs, a variety of p-type dopants have been used; each one has unique benefits depending on its electronic characteristics and interactions with the polymer as shown in Figure 7A. The EA of p-type dopants determines their efficiency in CP, which further governs charge

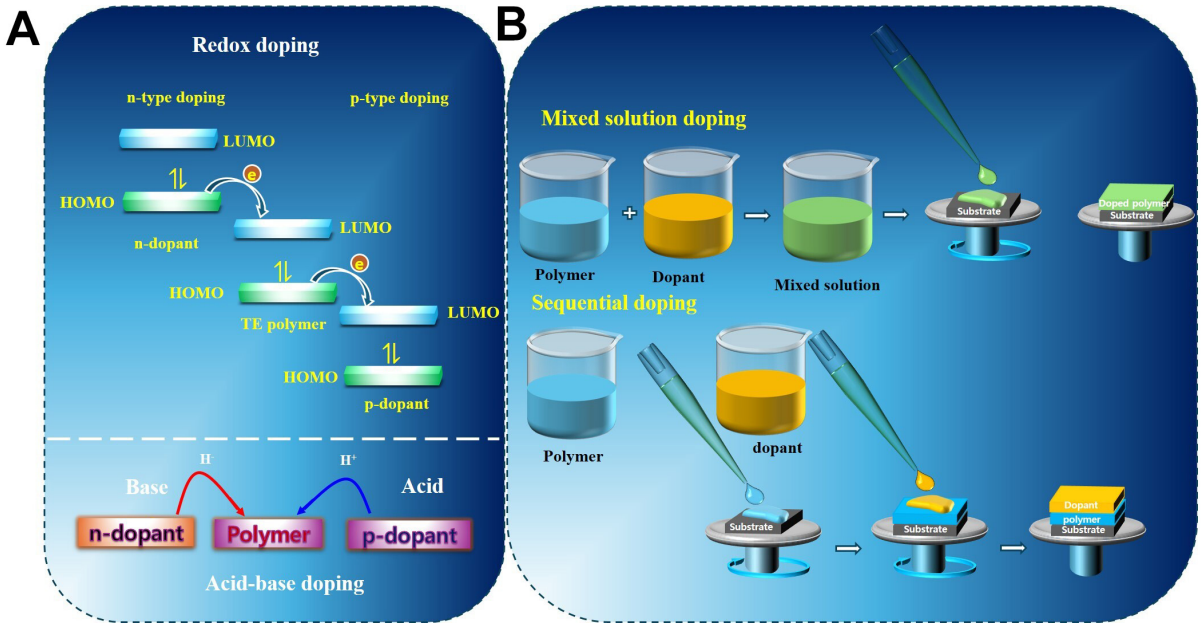

Figure 6. (A) Schematic illustration of redox and acid-base doping mechanisms in organic semiconductors. Redox doping involves charge transfer, while acid-base doping occurs via hydride ion or proton transfer; (B) Schematic illustration of mixed-solution doping and sequential doping approaches.

transfer efficiency during the doping process. Higher EA dopants are more suitable to accept electrons from the HOMO of the polymer, so oxidizing the polymer and raising hole concentration. The compound 2,3,5,6-tetrafluoro-7,7,8,8-tetracyanoquinodimethane (F4TCNQ) is a well-known p-type dopant due to its high EA, which plays a critical role in facilitating efficient p-type doping. Measuring at almost 5.25 eV, the improved EA of F4TCNQ is mostly attributed to the strong electron-withdrawing effects of the four fluorine atoms and four cyano groups symmetrically arranged around the TCNQ core[157]. F4TCNQ is a highly effective electron acceptor in redox doping systems since these substituents stabilize the LUMO. Moreover, changing the degree of fluorination on the molecule helps one to precisely adjust the EA of TCNQ derivatives. For instance, F1TCNQ and F2TCNQ, which include one and two fluorine atoms respectively, show lower EAs of roughly 5.01 eV and 5.10 eV, so reflecting a lower capacity to accept electrons than F4TCNQ. This tuning allows exact control over the charge transfer interactions with CP, so affecting the doping level and thermoelectric characteristics. Conversely, F6TCNNQ, a more highly fluorinated derivative, shows even more EA of roughly 5.37 eV, implying better doping potential because of its stronger electron-accepting properties[158].

Besides F4TCNQ, 2,3-dichloro-5,6-dicyano-1,4-benzoquinone (DDQ) is also extensively employed as a p-type dopant for hole-transporting polymers in organic electronic devices. When used with polymers such as P(g42T-T), DDQ has been said to provide comparable electrical performance as that obtained upon utilization of F4TCNQ[159]. The key benefit of DDQ is the fact that it is far less expensive, more than a hundred times less costly compared to F4TCNQ. A novel series of radialene-type dopants, including hexacyanotrimethylenecyclopropane (CN6-CP), has been synthesized with much greater electron affinities (~5.9 eV)[160]. CN6-CP is thus excellently suited to dope DPP-based copolymers and other polymers with very deeply lying HOMO levels. Doping with CN6-CP led to a dramatic increase of σ greater than 30 S cm^{-1}. Although CN6-CP offers advantages in performance, it lacks solubility in the majority of organic solvents, which restricts its practical applicability for solution-based doping processes. To get around this issue, scientists have created a derivative, TMCN3-CP, in which three of the nitrile groups are substituted with

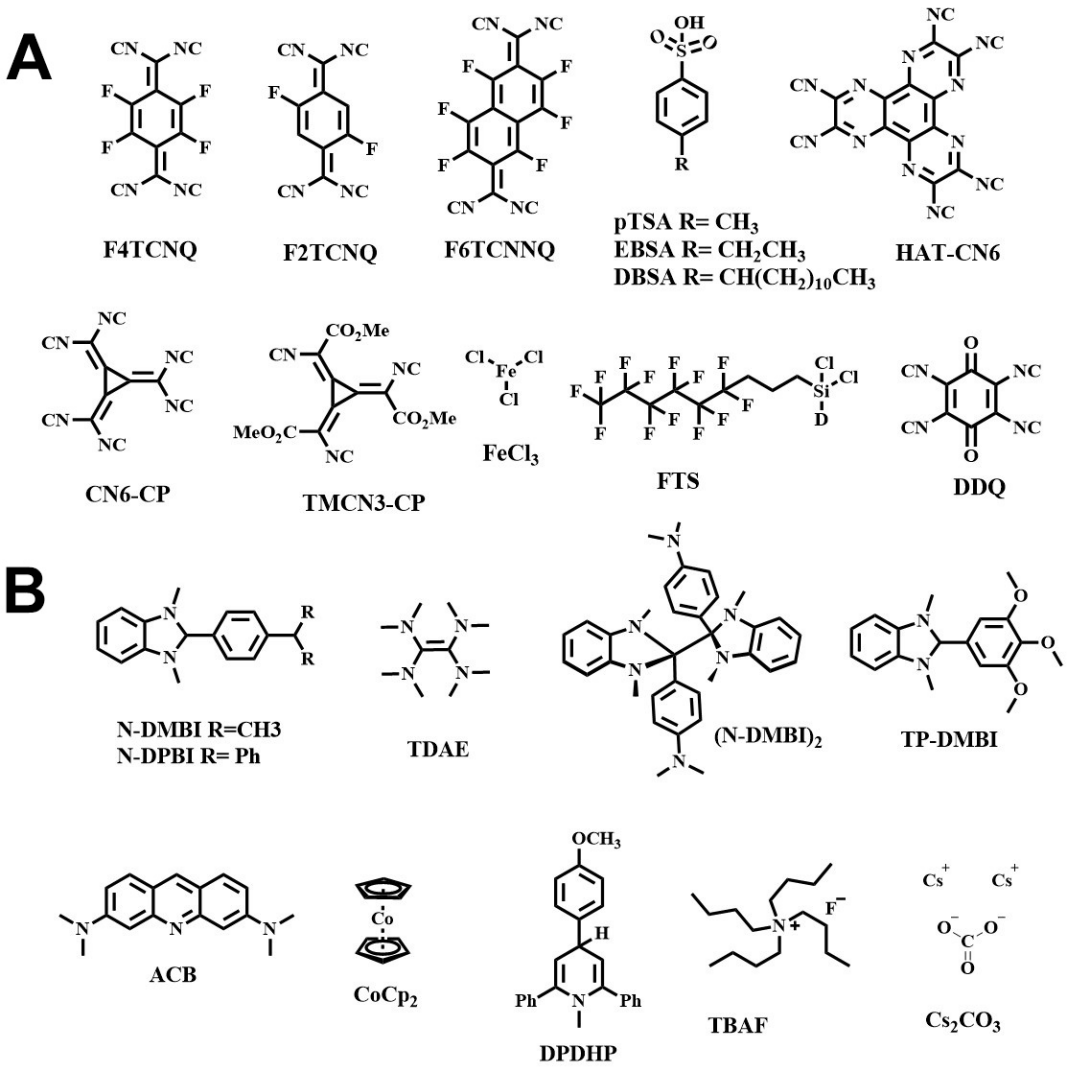

Figure 7. Chemical structures of common (A) p-type dopants and (B) n-type dopants.

methyl ester functional groups that greatly improve solubility[161].

Another foremost interesting dopant is $FeCl_3$, a popular inorganic oxidant that has proven to be an efficient and useful p-type dopant for numerous CP beyond typical systems such as P3HT and PEDOT. Recent studies have revealed it to be an exceptional doping efficiency in a family of DPP-based polymers such as PDPP-4T-EDOT, PDPSS-12T, PDPPSe-12T, and P29DPP-BTOM, all of which exhibit remarkable thermoelectric enhancements upon doping with $FeCl_3$. In such systems, $FeCl_3$ efficiently increases carrier concentration without disrupting the semi-crystalline arrangement of the polymer backbone necessary for sustaining effective charge transport and high σ. For instance, $FeCl_3$-doped PDPP-4T-EDOT was found to possess a PF of 298.2 μW m^{-1} K^{-2} and a conductivity of 272 S cm^{-1}, indicative of extremely high doping efficiency. Similarly, $FeCl_3$-doped PDPSS-12T and PDPPSe-12T showed PF of 178 μW m^{-1} K^{-2} and 364 μW m^{-1} K^{-2} and electrical conductivities of 318 S cm^{-1} and 997 S cm^{-1}, respectively. For P29DPP-BTOM, doping with $FeCl_3$ gave a PF of 195 μW m^{-1} K^{-2} and conductivity of 242.5 S cm^{-1}, further highlighting its broad-spectrum applicability in different polymer architectures.

In contrast to molecular redox dopants, acid dopants such as (tridecafluoro-1,1,2,2-tetrahydrooctyl)trichlorosilane (FTS), PTSA (p-toluenesulfonic acid), 4-ethylbenzenesulfonic acid (EBSA), and dodecylbenzenesulfonic acid (DBSA) operate via protonic (acid/base) doping methods and do not rely on EA-driven redox process. Successful p-type doping of the high-mobility polymer poly[2,5-bis(3-tetradecylthiophen-2-yl)thieno[3,2-b]thiophene] (PBTTT) with FTS and EBSA has been demonstrated, providing an insight into non-redox doping mechanisms[162]. FTS, specifically, functions via a protonation mechanism facilitated by acidic silanol groups produced upon hydrolysis, which form a self-assembled monolayer at the polymer surface and donate protons to the polymer backbone. This process enhances doping efficiency without compromising the structural integrity and stability of the film. Among, $FeCl_3$ has emerged as the most useful and powerful p-type dopant for DPP-based TE materials, due to its strong oxidative ability and the ability to enhance charge carrier concentration without disturbing the polymer's semi-crystalline order. In contrast to other molecular dopants such as F4TCNQ or CN6-CP, which are prone to solubility or miscibility limitations in certain backbones, $FeCl_3$ boasts remarkable compatibility in a broad variety of DPP structures. For instance, $FeCl_3$-doped PDPP-4T-EDOT, PDPSS-12T, PDPPSe-12T, and P29DPP-BTOM exhibit excellent TE performance. The improved performance is attributed to the ability of the dopant to penetrate deep-lying HOMO levels of the DPP units and introduce holes effectively, with the order of packing of the backbone for effective charge transfer.

n-type dopants

Effective n-type doping of OTE is essential to enhance σ, S, and thus the PF of CP. The chemical structure of common n-type dopants is shown in Figure 7B. Among the extensively studied dopants, N-DMBI is the most widely used n-type dopant. The E_{HOMO} of N-DMBI is -4.44 eV, which is lower in energy than the E_{LUMO} of typical n-type conjugated polymers, making direct electron transfer unfavorable thermodynamically. Instead, it follows other mechanisms of doping, mainly the hydrogen radical/electron transfer and hydride transfer mechanisms[120]. Thermal activation in the radical transfer mechanism enables cleavage of the C-H bond of N-DMBI to form a hydrogen radical and a neutral N-DMBI radical. The electron from the energy of singly occupied molecular orbitals E_{SOMO} (-2.23 eV) of the N-DMBI radical is subsequently transferred to the E_{LUMO} of the polymer, leading to the formation of a stable N-DMBI$^+$ cation. For the hydride transfer mechanism, a hydride ion (H^-) is heterolytically cleaved and transferred to the polymer. The two mechanisms are energetically demanding, with enthalpy changes of 80.2 and 74.6 kcal mol^{-1} for the formation of neutral hydrogen and hydride, respectively. Thus, thermal treatment (typically 80-180 °C) is required to initiate doping and the efficiency is highly sensitive to the chemical structure of the polymer[121-123]. In an attempt to overcome the solubility and miscibility problem of N-DMBI with polymers, scientists have synthesized many molecular derivatives. One of these is N-DPBI (4-(1,3-dimethyl-2,3-dihydro-1H-benzimidazol-2-yl)-N,N-diphenylaniline), wherein the dimethylamino group in N-DMBI is replaced with a diphenylamino substituent[163]. This modification was performed to stabilize the radical species via resonance by phenyl rings. However, despite structural modification, N-DPBI showed similar conductivity (σ ~4 × 10^{-3} S cm^{-1}) to that of N-DMBI (~8 × 10^{-3} S cm^{-1}) when used to dope N2200, largely due to poor miscibility of dopants in the polymer matrix. TP-DMBI is another novelty where a 3,4,5-trimethoxyphenyl unit is introduced into the N-DMBI backbone to enhance miscibility as well as electron-donating capability[124]. Further, a dimeric species of N-DMBI, $(N\text{-}DMBI)_2$, which had the advantages of strong reducing ability and small cation size, was synthesized to deliver two electrons directly to the polymer and form two N DMBI$^+$ cations. This pathway significantly enhances doping efficiency with σ ~8 S cm^{-1} in flouro-benzodifurandione-phenylenevinylene (FBDPPV) using only 10.7 mol% of $(N\text{-}DMBI)_2$, while 43 mol% monomeric N-DMBI is required to achieve similar performance[164]. Other notable n-type dopants include Tetrakis(dimethylamino)ethylene (TDAE), a highly volatile compound with four electron-donating amine groups connected by a central C=C bond with strong π-electron donating nature. The high reducing ability of TDAE is advantageous for efficient doping in the vapor phase with conductivities of 2.4-

7.8 S cm^{-1} having been reported[129,139,165]. Its volatility renders it difficult to manage doping, and doped systems are found to be unstable even under inert conditions, thereby limiting long-term application[166]. In contrast, tetrabutylammonium salts (TBAX, X = F^-, OH^-, CH_3COO^-, *etc.*) provide a more solution-processable and stable pathway. For instance, tetrabutylammonium fluoride (TABF) reacts with electron-deficient polymers such as chloro-benzodifurandione-phenylenevinylene (ClBDPPV) to give (polymer-F^-) complexes that act as electron donors[167]. Annealing 25 mol% TBAF-doped ClBDPPV films at 130 °C for 12 h produced σ of 0.62 S cm^{-1}, demonstrating exceptional air stability, maintaining greater than 0.1 S cm^{-1} after one week. Among them, N-DMBI remains the most effective and versatile dopant, especially in doping DPP-based thermoelectric polymers. Recent studies have demonstrated the ability of DPP-based polymers such as P(PzDPP-CT2), PTz-5-DPP, ThDPP-CNBTz, and pDFSe, all of which were doped effectively with N-DMBI. These polymers have exhibited superior TE performance due to their electron-deficient backbones, strong intermolecular interactions, and good doping compatibility. For instance, P(PzDPP-CT2) has pyrazine and cyano-functionalized bithiophene moieties, which provide σ = 8.4 S cm^{-1} and PF = 57.3 μW m^{-1} K^{-2}. PTz-5-DPP, synthesized via oxidative direct arylation polycondensation, provides a very high PF value of ~106.0 μW m^{-1} K^{-2}. Even more impressively, ThDPP-CNBTz with a thiophene-flanked DPP backbone provides σ = 50.6 S cm^{-1} and PF = 126.8 μW m^{-1} K^{-2} upon N-DMBI doping. But the most surprising performance comes with pDFSe, a noncovalently fused-ring-designed polymer, that facilitates charge transport in disordered films with a record-high value of σ at 62.6 S cm^{-1} and PF of 133.1 μW m^{-1} K^{-2}. The results show that it is the cooperation of well-designed polymer architectures and good n-dopants such as N-DMBI that provide the solution for further improving organic TE devices.

The air stability of n-type CP remains a challenge for its practical application in OTEs. Unlike their p-type counterparts, the majority of n-type polymers are stable under inert atmospheres only since organic anions, particularly carbanions, are susceptible to oxidative degradation. The reaction rapidly quenches mobile electrons and decreases σ[128,168]. One of the potential approaches for preventing this problem is the synthesis of polymers with deep levels of LUMO (typically lower than -4.7 eV), reducing energy offset to oxidative degradation[169,170]. In order to get over this, strategies such as locating electron-deficient groups on the polymer backbone and employing dopants that form stable charge-transfer complexes have proven useful. For instance, recently, PTz-DPP-based TE polymers have shown deepened LUMO levels with higher nitrogen content which directly affect the DOS, making it easier for polaron formation and leading to improved charge transport properties[151]. In addition, designing a thicker dopant or film layer enriched on the surface might utilize a self-encapsulation effect, preventing physical oxygen and moisture entry. For example, 3-8 μm thick ClBDPPV films doped with 25 mol% TBAF retained over 0.1 S cm^{-1} conductivity even after exposure to air for one week, showing the potential of combinations of low-LUMO polymers with stable dopants[167]. In combination, synergistic polymer chemistry design, dopant selection, and film morphology are required to achieve both high performance and stable durability for n-type OTE materials.

COMPARATIVE STUDY ON DPP-BASED THERMOELECTRIC POLYMERS

Comparative study in p-type DPP-based thermoelectric polymers

In a comparative study of p-type DPP-based thermoelectric polymers, PDPP-4T-EDOT, PDPPSe-12 and P29DPP-BTOM emerge as potential candidates, each excelling in different performance metrics. PDPP-4T-EDOT realizes a remarkably high PF of 298.2 μW m^{-1} K^{-2} at an optimal doping concentration of 0.5 mM. This work highlights that the incorporation of electron-rich EDOT moiety into a DPP framework results in significant enhancement of the electronic characteristics of the polymer, significantly outpacing other contenders such as PDPP-3T and P29DPP-BTOM. The EDOT incorporation increases the HOMO levels, allowing efficient p-doping without sacrificing high coplanarity and charge carrier transport characteristics. PDPPSe-12 is a selenium-substituted DPP-selenophene copolymer with strong intermolecular forces and stable morphology due to the larger atomic radius of selenium. PDPPSe-12 exhibited high hole mobility

(~7 $cm^2 V^{-1} s^{-1}$) and exceptional σ (~997 S cm^{-1}) after doping with $FeCl_3$, which was higher than its sulfur analog. It reached a PF of 364 μW $m^{-1} K^{-2}$ and a record ZT of 0.25 at low doping levels, demonstrating its potential to develop high-performance organic TE materials.

Similarly, the methoxy-functionalized P29DPP-BTOM exhibits a remarkable PF of 195 μW $m^{-1} K^{-2}$, which is substantiated by the judicious introduction of methoxy groups in the polymer backbone. These methoxy substituents increase the lamellar stacking distance of the polymer matrix and thus allow the dopant diffusion in a more effective way, directly increasing the doping efficiency, especially for larger dopants, including FeCl3. P29DPP-BTOM exhibits excellent σ up to 242.4 S cm^{-1} with a high S. Optimization of TE performance requires such a balance between conductivity and S, and thus P29DPP-BTOM becomes a strong competitor in this field. In comparison, although some other polymers, such as PDPP3T, also show excellent properties in regard to hole mobility and σ, the overall thermoelectric efficiency is less than PDPP-4T-EDOT. For instance, although PDPP3T has good performance in organic thin-film transistors, it only yields a high PF of 276 μW $m^{-1} K^{-2}$ under optimal doping conditions, which is still lower than that of PDPP-4T-EDOT.

However, P29DPP-BTOM's design illustrates the effectiveness of structural optimization to enhance doping efficiency and mobility and also underlines the importance of tailored strategies in polymer design for optimizing TE materials. The comparative study of σ and PF of DPP-based p-type thermoelectric polymers over time is shown in Figure 8A and chemical structures of the high performance p-type thermoelectric polymer are shown in Figure 8B.

Comparative study in n-type DPP-based thermoelectric polymers

In the search for advanced n-type thermoelectric polymers, several novel materials have emerged, each demonstrating unique structural features and electron-transport properties. Among these, the significant examples are P(PzDPP-CT2), PTz-5-DPP, ThDPP-CNBTz, PTz-DPP and pDFSe. The compound P(PzDPP-CT2), which incorporates pyrazine groups and cyano-functionalized bithiophene, has shown an excellent σ of 8.4 S cm^{-1} and a PF of 57.3 μW $m^{-1} K^{-2}$. Such performance indicates a remarkable EA and effective charge transport, which is supported by intramolecular hydrogen bonding interactions. PTz-5-DPP, synthesized through oxidative direct arylation polycondensation, exhibited strikingly high capabilities with σ over 8.38 S cm^{-1} and a PF close to 106.0 μW $m^{-1} K^{-2}$, illustrating the advantages of efficient synthesis for practical applications. On the other side, ThDPP-CNBTz, PTz-DPP and pDFSe also show excellent thermoelectric properties. ThDPP-CNBTz, with a thiophene-flanked DPP backbone, showed a high σ of 50.6 S cm^{-1} and a PF of 126.8 μW $m^{-1} K^{-2}$ after n-doping, thus showing high potential for flexible devices. Similarly, PTz-DPP in a recent study by increasing the nitrogen content in the polymer backbones and using amphipathic side chains, the compound shows enhanced solubility, morphology, and doping efficiency with the n-type dopant N-DMBI of the polymers. With higher nitrogen content, the DOS at the Fermi level increased, making it easier for polaron formation and leading to improved charge transport properties. PTz-DPP exhibited superior performance with high σ (63.8 S cm^{-1}), and PF of 111.8 μW $m^{-1} K^{-2}$ because of negligible structural perturbation, retained molecular order, and hopping to band-like charge transport transition. On the other hand, pDFSe, based on a noncovalently fused-ring design, showed a remarkably high conductivity of 62.6 S cm^{-1} and the best PF of 133.1 μW $m^{-1} K^{-2}$, indicating its efficacy in facilitating charge-carrier mobility in amorphous structures. While individual polymers each have their own respective advantages, the remarkably high PF of pDFSe positions it at the forefront of n-type organic TE materials, making it a promising candidate for future applications. In general, this comparative study demonstrates that pDFSe not only beats others but also marks an essential development in the evolution of n-type TE materials. The comparative study of σ and PF of DPP-based n-type TE polymers over time is shown in Figure 9A and chemical structures of the high performance p-type thermoelectric polymer are

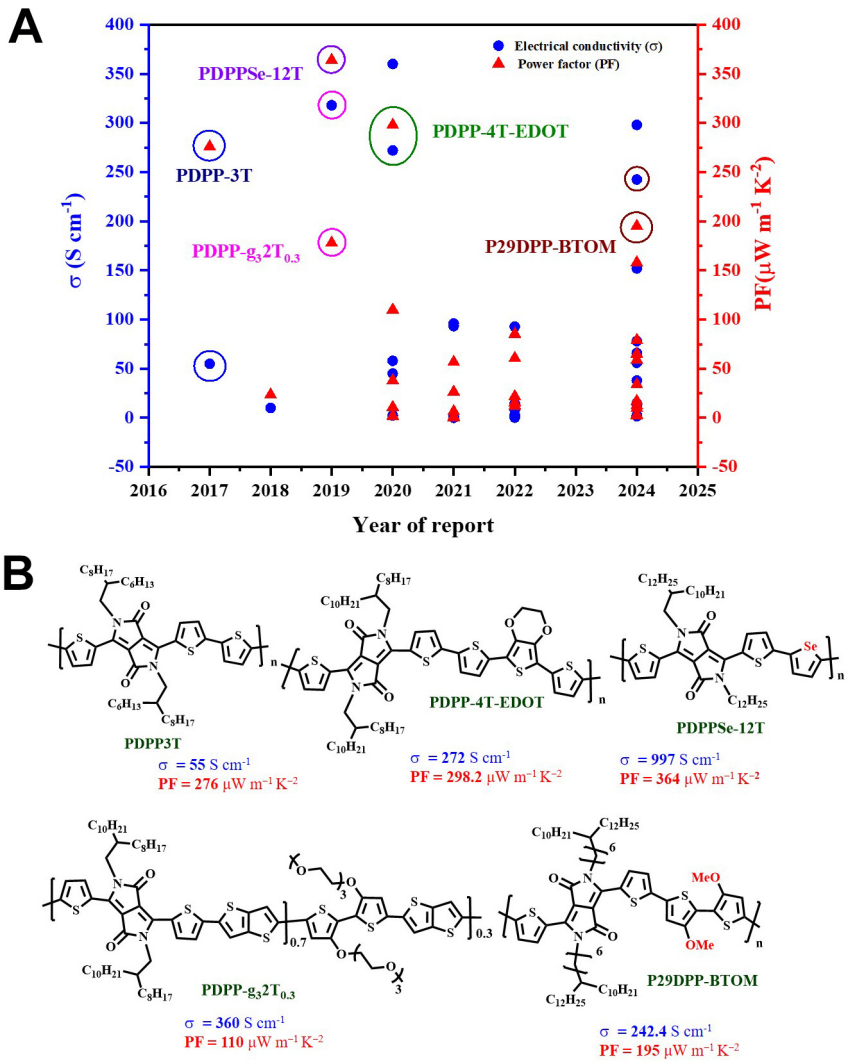

Figure 8. (A) Comparative analysis of the progress in electrical conductivity and PF of DPP-based p-type thermoelectric polymers reported over time and (B) Chemical structures of representative high-performance p-type thermoelectric polymers, showcasing key structural features contributing to enhanced TE properties. PF: Power factor; TE: thermoelectric; DPP:

shown in Figure 9B.

From the literature discussed, several strategies have been identified to overcome low TE performance. Firstly, the synthesis of electron-deficient backbones such as DPP-based polymers lowers LUMO energy levels and facilitates better n-doping thermodynamics. For instance, the DPP-based copolymer P(PzDPP-CT2) showed high σ of 8.4 S cm^{-1} and PF of 57.3 μW m^{-1} K^{-2}, which indicates improved n-type doping efficiency due to its well-structured molecular architecture. Second, dopant design advancements, particularly with N-DMBI derivatives such as TP-DMBI and $(N\text{-DMBI})_2$, have improved doping efficiency through improved dopant-polymer miscibility, enhanced radical stability, and promotion of multielectron transfer. Moreover, the unprecedented enhancement of n-type polymer TE performance by the design of pDFSe with a noncovalently fused-ring structure with lower CCL 26.4 Å, higher paracrystalline disorder (g = 21%), and more planar surface morphology. These features enhance doping efficiency so that pDFSe can show a high electron mobility of 6.15 cm^2 V^{-1} s^{-1} and, upon n-doping, an exceptional σ of 62.6 S cm^{-1} and a

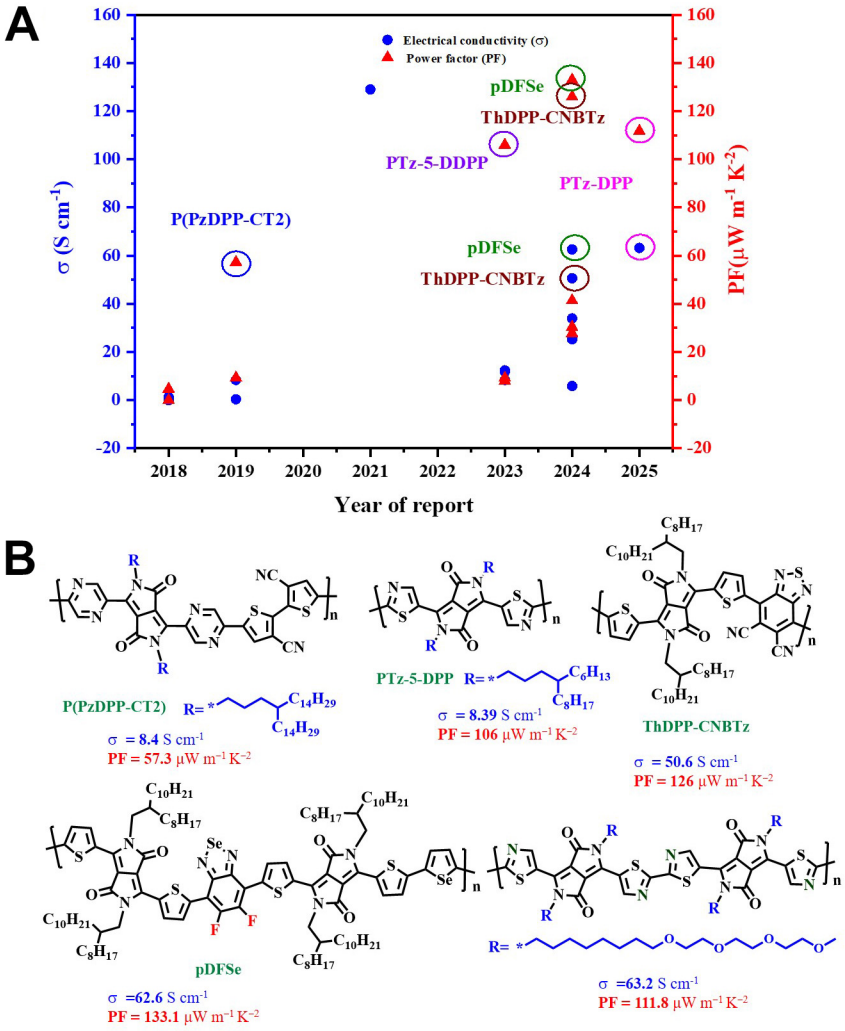

Figure 9. (A) Comparative analysis of the progress in electrical conductivity and PF of DPP-based n-type thermoelectric polymers reported over time and (B) Chemical structures of representative high-performance n-type thermoelectric polymers. PF: Power factor; DPP:

PF of 133.1 μW m^{-1} K^{-2}. These findings in aggregate indicate a clear direction forward in the development of high-performance n-type TE materials and illustrate the necessity of dopant polymer synergy.

CONCLUSION AND OUTLOOK

In this review, we provided an overview of recent advances in organic TE materials, more precisely based on the DPP p-type and n-type thermoelectric conjugated polymers as DPP has proven to be an extremely promising building block in the preparation of state-of-the-art OTE materials. Its unique electronic features, including a strong electron-accepting tendency, high planarity, and good thermal stability, have enabled the advancement in p-type and n-type materials with a significantly enhanced TE performance. Molecular design strategies for OTE materials are evolving from simply optimizing σ, S, and κ, toward a deeper understanding of the structure-property-performance relationships at the molecular level. For DPP-based systems, particularly, fine-tuning these interdependent parameters through rational backbone and side-chain engineering is essential for achieving high-performance p and n-type materials. The significant advancements in TE performance will stem from systematic investigations into how molecular polarity,

energy level alignment, backbone rigidity, and intermolecular interactions influence doping behavior. For instance, the P(PzDPP-CT2) and P(PzDPP-2FT) polymers developed by Yan *et al.*[123,145] showcase that introducing electron-deficient pyrazine units and noncovalent interactions can enhance backbone planarity, improve electron mobility, and sustain structural order even under high doping levels critical for long-term stability. Similarly, polymers such as PDCNBT-DPP and PDCNBSe-DPP demonstrate deep-lying LUMOs and reduced aromaticity from Se substitution yield significant improvements in conductivity and PF. These examples highlight the need for rational design of DPP derivatives that can simultaneously achieve low energy levels, high mobility, and doping resilience. Furthermore, as shown by the work on PTz-5-DPP and P(DPP-DCNPz), low-crystallinity systems with mixed packing or transitional morphologies can offer better dopant accommodation without large aggregate formation, contributing to stable high-performance TE behavior. Very recently, the incorporation of electron-deficient heterocycles with high sp^2-N content, as in PTz-DPP, effectively modulates the DOS near the Fermi level, promoting band-like charge transport and significantly enhancing ZT. Moreover, p-type materials have shown excellent PFs, at times over 200 μW m^{-1} K^{-2}, which is much better than many conventional p-type polymers and other conjugated polymers. n-type materials have also seen significant improvement, with some polymers reaching PFs of over 100 μW m^{-1} K^{-2}. In the realm of p-type materials, PDPP-4T-EDOT has distinguished itself with an impressive PF of 298.2 μW m^{-1} K^{-2} at an optimal doping concentration of 0.5 mM. In parallel, the methoxy-functionalized P29DPP-BTOM achieved a commendable PF of 195 μW m^{-1} K^{-2}, illustrating the importance of structural modifications to optimize doping efficiency and mobility. For n-type DPP-based materials, pDFSe stands out with a remarkable PF of 133.1 μW m^{-1} K^{-2}, marking a significant milestone in the development of n-type thermoelectric polymers. However, despite these advances, several key challenges and opportunities remain. Further research in this regard is important to enhance the performance of n-type and, in particular, to achieve efficiency levels comparable to or higher than those of p-type materials. The trade-off between σ and the S remains a significant challenge, and therefore efforts in molecular engineering and nano structuring are well justified to optimize this trade-off.

Overall, DPP-based materials are a promising candidate for efficient organic TE materials. The insights gained from the comparative studies of p-type and n-type materials pave the way for optimizing these promising TE materials. Although significant progress has been made in enhancing the thermoelectric properties of DPP-based polymers, their implementation in practical devices such as flexible thermoelectric modules or wearable energy harvesters remains limited. Future research should focus on scalable processing techniques and device fabrication strategies to translate these promising materials into real-world applications. Continued research and development in this field is expected to lead to significant advances in the field.

DECLARATIONS

Authors' contributions

Proposed the topic of this review: Kim, Y. H.
Manuscript writing: Girase, J. D.; Kim, Y. H.
Data curation: Girase, J. D.; Kim, I. C.

Availability of data and materials

Not applicable.

Financial support and sponsorship

This research was supported by the National Research Foundation (NRF) of Korea (Grant numbers RS-2023-00301974, RS-2024-00336766 and RS-2024-00406548).

Conflicts of interest

Kim Y. H. is an Editorial board member of the journal *Energy Materials* and was not involved in any part of the editorial process, including reviewer selection, manuscript handling, or decision-making. The other authors declare that they have no conflicts of interest.

Ethical approval and consent to participate

Not applicable.

Consent for publication

Not applicable.

Copyright

REFERENCES

1. Dincer, I. Renewable energy and sustainable development: a crucial review. *Renew. Sustain. Energy. Rev.* **2000**, *4*, 157-75. DOI
2. Fitriani; Ovik, R.; Long, B.; et al. A review on nanostructures of high-temperature thermoelectric materials for waste heat recovery. *Renew. Sustain. Energy. Rev.* **2016**, *64*, 635-59. DOI
3. Snyder, G. J.; Toberer, E. S. Complex thermoelectric materials. *Nat. Mater.* **2008**, *7*, 105-14. DOI PubMed
4. Kim, Y. J.; Gu, H. M.; Kim, C. S.; et al. High-performance self-powered wireless sensor node driven by a flexible thermoelectric generator. *Energy* **2018**, *162*, 526-33. DOI
5. vom Boegel, G.; Meyer, F.; Kemmerling, M. Wireless sensor system for industrial applications powered by thermoelectric generator. In *Smart SysTech 2014; European Conference on Smart Objects, Systems and Technologies*. IEEE, 2014: 1-5. DOI
6. Yang, Y.; Wei, X.; Liu, J. Suitability of a thermoelectric power generator for implantable medical electronic devices. *J. Phys. D. Appl. Phys.* **2007**, *40*, 5790. DOI
7. Weber, J.; Potje-kamloth, K.; Haase, F.; Detemple, P.; Völklein, F.; Doll, T. Coin-size coiled-up polymer foil thermoelectric power generator for wearable electronics. *Sensors. Actuators. A. Phys.* **2006**, *132*, 325-30. DOI
8. Wu, W.; Du, Z.; Cui, J.; Shi, Z.; Deng, Y. Thermoelectric generator used in fire-alarm temperature sensing. *J. Electron. Mater.* **2015**, *44*, 1851-7. DOI
9. Shi, Y.; Wang, Y.; Deng, Y.; et al. A novel self-powered wireless temperature sensor based on thermoelectric generators. *Energy. Convers. Manag.* **2014**, *80*, 110-6. DOI
10. Dughaish, Z. Lead telluride as a thermoelectric material for thermoelectric power generation. *Phys. B. Condens. Matter.* **2002**, *322*, 205-23. DOI
11. Goldsmid, H. J. The electrical conductivity and thermoelectric power of bismuth telluride. *Proc. Phys. Soc.* **1958**, *71*, 633. DOI
12. Boukai, A. I.; Bunimovich, Y.; Tahir-Kheli, J.; Yu, J. K.; Goddard, W. A. I. I. I.; Heath, J. R. Silicon nanowires as efficient thermoelectric materials. *Nature* **2008**, *451*, 168-71. DOI
13. Zhao, L. D.; Lo, S. H.; Zhang, Y.; et al. Ultralow thermal conductivity and high thermoelectric figure of merit in SnSe crystals. *Nature* **2014**, *508*, 373-7. DOI
14. Gayner, C.; Kar, K. K. Recent advances in thermoelectric materials. *Prog. Mater. Sci.* **2016**, *83*, 330-82. DOI
15. Bulusu, A.; Walker, D. Review of electronic transport models for thermoelectric materials. *Superlattices. Microstructur.* **2008**, *44*, 1-36. DOI
16. Venkatasubramanian, R.; Siivola, E.; Colpitts, T.; O'Quinn, B. Thin-film thermoelectric devices with high room-temperature figures of merit. *Nature* **2001**, *413*, 597-602. DOI PubMed
17. Pei, Y.; Shi, X.; LaLonde, A.; Wang, H.; Chen, L.; Snyder, G. J. Convergence of electronic bands for high performance bulk thermoelectrics. *Nature* **2011**, *473*, 66-9. DOI
18. Blackburn, J. L.; Ferguson, A. J.; Cho, C.; Grunlan, J. C. Carbon-nanotube-based thermoelectric materials and devices. *Adv. Mater.* **2018**, *30*, 1704386. DOI PubMed
19. Zhou, S.; Shi, X. L.; Li, L.; et al. Advances and outlooks for carbon nanotube-based thermoelectric materials and devices. *Adv. Mater.* **2025**, *37*, 2500947. DOI
20. Bubnova, O.; Khan, Z. U.; Malti, A.; et al. Optimization of the thermoelectric figure of merit in the conducting polymer poly(3,4-ethylenedioxythiophene). *Nat. Mater.* **2011**, *10*, 429-33. DOI
21. Zhou, D.; Zhang, H.; Zheng, H.; et al. Recent advances and prospects of small molecular organic thermoelectric materials. *Small* **2022**, *18*, 2200679. DOI
22. Lee, S.; Kim, S.; Pathak, A.; et al. Recent progress in organic thermoelectric materials and devices. *Macromol. Res.* **2020**, *28*, 531-52. DOI
23. Glaudell, A. M.; Cochran, J. E.; Patel, S. N.; Chabinyc, M. L. Impact of the doping method on conductivity and thermopower in

semiconducting polythiophenes. *Adv. Energy. Mater.* **2015**, *5*, 1401072. DOI

24. Russ, B.; Glaudell, A.; Urban, J. J.; Chabinyc, M. L.; Segalman, R. A. Organic thermoelectric materials for energy harvesting and temperature control. *Nat. Rev. Mater.* **2016**, *1*, 201650. DOI
25. Zhang, Q.; Sun, Y.; Xu, W.; Zhu, D. Organic thermoelectric materials: emerging green energy materials converting heat to electricity directly and efficiently. *Adv Mater* 2014;26:6829-51. DOI
26. Patel, S. N.; Glaudell, A. M.; Peterson, K. A.; et al. Morphology controls the thermoelectric power factor of a doped semiconducting polymer. *Sci. Adv.* **2017**, *3*, e1700434. DOI PubMed PMC
27. Li, W.; Hendriks, K. H.; Wienk, M. M.; Janssen, R. A. Diketopyrrolopyrrole polymers for organic solar cells. *Acc. Chem. Res.* **2016**, *49*, 78-85. DOI PubMed
28. Cheon, H. J.; An, T. K.; Kim, Y. Diketopyrrolopyrrole (DPP)-based polymers and their organic field-effect transistor applications: a review. *Macromol. Res.* **2022**, *30*, 71-84. DOI
29. Nielsen, C. B.; Turbiez, M.; McCulloch, I. Recent advances in the development of semiconducting DPP-containing polymers for transistor applications. *Adv. Mater.* **2013**, *25*, 1859-80. DOI PubMed
30. Kang, I.; An, T. K.; Hong, J. A.; et al. Effect of selenophene in a DPP copolymer incorporating a vinyl group for high-performance organic field-effect transistors. *Adv. Mater.* **2013**, *25*, 524-8. DOI
31. Lee, J. H.; Lee, Y. H.; Ha, Y. H.; et al. Semiconducting/insulating polymer blends with dual phase separation for organic field-effect transistors. *RSC. Adv.* **2017**, *7*, 7526-30. DOI
32. Sassi, M.; Buccheri, N.; Rooney, M.; et al. Near-infrared roll-off-free electroluminescence from highly stable diketopyrrolopyrrole light emitting diodes. *Sci. Rep.* **2016**, *6*, 34096. DOI PubMed PMC
33. Li, Y.; Li, H.; Chen, H.; et al. Controlling crystallite orientation of diketopyrrolopyrrole-based small molecules in thin films for highly reproducible multilevel memory device: role of furan substitution. *Adv. Funct. Mater.* **2015**, *25*, 4246-54. DOI
34. Chen, C.; Lee, W.; Shen, T.; et al. Highly reliable and sensitive tactile transistor memory. *Adv. Elect. Mater.* **2017**, *3*, 1600548. DOI
35. Zhou, Y.; Han, S. T.; Yan, Y.; et al. Ultra-flexible nonvolatile memory based on donor-acceptor diketopyrrolopyrrole polymer blends. *Sci. Rep.* **2015**, *5*, 10683. DOI PubMed PMC
36. Kaur, M.; Lee, D. H.; Yang, D. S.; et al. Diketopyrrolopyrrole-bitellurophene containing a conjugated polymer and its high performance thin-film transistor sensor for bromine detection. *Chem. Commun.* **2014**, *50*, 14394-6. DOI
37. Surya, S. G.; Nagarkar, S. S.; Ghosh, S. K.; Sonar, P.; Ramgopal, R. V. OFET based explosive sensors using diketopyrrolopyrrole and metal organic framework composite active channel material. *Sens. Actuators. B. Chem.* **2016**, *223*, 114-22. DOI
38. Wang, B.; Huynh, T. P.; Wu, W.; et al. A highly sensitive diketopyrrolopyrrole-based ambipolar transistor for selective detection and discrimination of xylene isomers. *Adv. Mater.* **2016**, *28*, 4012-8. DOI
39. Casutt, M.; Ruscello, M.; Strobel, N.; et al. Diketopyrrolopyrrole-polymer meets thiol-ene click chemistry: a cross-linked acceptor for thermally stable near-infrared photodetectors. *Chem. Mater.* **2019**, *31*, 7657-65. DOI
40. Hu, L.; Qiao, W.; Zhou, X.; et al. Side-chain engineering for fine-tuning of molecular packing and nanoscale blend morphology in polymer photodetectors. *Polym. Chem.* **2017**, *8*, 2055-62. DOI
41. Liu, Q.; Kanahashi, K.; Matsuki, K.; et al. Triethylene glycol substituted diketopyrrolopyrrole- and isoindigo-dye based donor-acceptor copolymers for organic light-emitting electrochemical cells and transistors. *Adv. Elect. Mater.* **2020**, *6*, 1901414. DOI
42. Qu, S.; Tian, H. Diketopyrrolopyrrole (DPP)-based materials for organic photovoltaics. *Chem. Commun.* **2012**, *48*, 3039-51. DOI PubMed
43. Liu, Q.; Sun, H.; Ponnappa, S. P.; et al. Naphthalene flanked diketopyrrolopyrrole: a new DPP family member and its comparative optoelectronic properties with thiophene- and furan- flanked DPP counterparts. *Org. Electron.* **2019**, *74*, 290-8. DOI
44. Liu, Q.; Sun, H.; Blaikie, C.; et al. Naphthalene flanked diketopyrrolopyrrole based organic semiconductors for high performance organic field effect transistors. *New. J. Chem.* **2018**, *42*, 12374-85. DOI
45. Liu, Q.; Chavhan, S.; Zhang, H.; et al. Short Alkyl chain engineering modulation on naphthalene flanked diketopyrrolopyrrole toward high-performance single crystal transistors and organic thin film displays. *Adv. Elect. Mater.* **2021**, *7*, 2000804. DOI
46. Luo, N.; Zhang, G.; Liu, Z. Keep glowing and going: recent progress in diketopyrrolopyrrole synthesis towards organic optoelectronic materials. *Org. Chem. Front.* **2021**, *8*, 4560-81. DOI
47. Loser, S.; Lou, S. J.; Savoie, B. M.; et al. Systematic evaluation of structure-property relationships in heteroacene -diketopyrrolopyrrole molecular donors for organic solar cells. *J. Mater. Chem. A.* **2017**, *5*, 9217-32. DOI
48. Bürgi, L.; Turbiez, M.; Pfeiffer, R.; Bienewald, F.; Kirner, H.; Winnewisser, C. High-mobility ambipolar near-infrared light-emitting polymer field-effect transistors. *Adv. Mater.* **2008**, *20*, 2217-24. DOI
49. Li, Y.; Sonar, P.; Murphy, L.; Hong, W. High mobility diketopyrrolopyrrole (DPP)-based organic semiconductor materials for organic thin film transistors and photovoltaics. *Energy. Environ. Sci.* **2013**, *6*, 1684-710. DOI
50. Tang, A.; Zhan, C.; Yao, J.; Zhou, E. Design of diketopyrrolopyrrole (DPP)-based small molecules for organic-solar-cell applications. *Adv. Mater.* **2017**, *29*, 1600013. DOI PubMed
51. Yi, Z.; Wang, S.; Liu, Y. Design of high-mobility diketopyrrolopyrrole-based π-conjugated copolymers for organic thin-film transistors. *Adv. Mater.* **2015**, *27*, 3589-606. DOI
52. Naik, M. A.; Patil, S. Diketopyrrolopyrrole-based conjugated polymers and small molecules for organic ambipolar transistors and solar cells. *J. Polym. Sci. Part. A:. Polym. Chem.* **2013**, *51*, 4241-60. DOI
53. Chandran, D.; Lee, K. Diketopyrrolopyrrole: a versatile building block for organic photovoltaic materials. *Macromol. Res.* **2013**, *21*,

272-83. DOI

54. Grzybowski, M.; Gryko, D. T. Diketopyrrolopyrroles: synthesis, reactivity, and optical properties. *Adv. Opt. Mater.* **2015**, *3*, 280-320. DOI
55. Dou, L.; Liu, Y.; Hong, Z.; Li, G.; Yang, Y. Low-bandgap near-IR conjugated polymers/molecules for organic electronics. *Chem. Rev.* **2015**, *115*, 12633-65. DOI
56. Kim, C.; Liu, J.; Lin, J.; et al. Influence of structural variation on the solid-state properties of diketopyrrolopyrrole-based oligophenylenethiophenes: single-crystal structures, thermal properties, optical bandgaps, energy levels, film morphology, and hole mobility. *Chem. Mater.* **2012**, *24*, 1699-709. DOI
57. Beretta, D.; Neophytou, N.; Hodges, J. M.; et al. Thermoelectrics: from history, a window to the future. *Mater. Sci. Eng. R. Rep.* **2019**, *138*, 100501. DOI
58. Seebeck, T. J. *Magnetische polarisation der metalle und erze durch temperatur-differenz*; W. Engelmann, 1895. https://books.google.com/books?id=1u0ZWscprXkC&dq=58.+Seebeck+TJ.+Magnetische+Polarisation+Der+Metalle+Und+Erze+Durch+Temperatur-Differenz%3B+W.+Engelmann,+1895.%5BDOI:10.1002/andp.18260820102%5D&lr=&hl=zh-CN&source=gbs_navlinks_s (accessed 2025-05-30).
59. Rowe, D. M. *CRC Handbook of thermoelectrics*, 1th ed.; CRC Press, 2018. DOI
60. Du, Y.; Cai, K.; Chen, S.; et al. Thermoelectric fabrics: toward power generating clothing. *Sci. Rep.* **2015**, *5*, 6411. DOI PubMed PMC
61. Peltier, J. C. A. Investigation of the heat developed by electric currents in homogeneous materials and at the junction of two different conductors. *Ann. Chim. Phys.* **1834**, *56*, 371. Available from: https://archive.org/details/s3id13208250. [Last accessed on 2 July 2025].
62. Peltier, J. C. A. Nouvelles experiences sur la caloricite des courans electriques. *Ann. Chim. Phys.* 1834. Available from: https://www.foldvaribooks.com/pages/books/769/jean-charles-athanase-peltier/nouvelles-experiences-sur-la-caloricite-des-courans-electriques. [Last accessed on 1 July 2025].
63. Ohta, H.; Kim, S.; Mune, Y.; et al. Giant thermoelectric Seebeck coefficient of a two-dimensional electron gas in $SrTiO_3$. *Nat. Mater.* **2007**, *6*, 129-34. DOI
64. Heremans, J. P.; Jovovic, V.; Toberer, E. S.; et al. Enhancement of thermoelectric efficiency in PbTe by distortion of the electronic density of states. *Science* **2008**, *321*, 554-7. DOI
65. Snyder, G. J.; Snyder, A. H. Figure of merit ZT of a thermoelectric device defined from materials properties. *Energy. Environ. Sci.* **2017**, *10*, 2280-3. DOI
66. Dresselhaus, M.; Chen, G.; Tang, M.; et al. New directions for low-dimensional thermoelectric materials. *Adv. Mater.* **2007**, *19*, 1043-53. DOI
67. Yoon, C.; Reghu, M.; Moses, D.; et al. Hopping transport in doped conducting polymers in the insulating regime near the metal-insulator boundary: polypyrrole, polyaniline and polyalkylthiophenes. *Synth. Met.* **1995**, *75*, 229-39. DOI
68. Mateeva, N.; Niculescu, H.; Schlenoff, J.; Testardi, L. R. Correlation of seebeck coefficient and electric conductivity in polyaniline and polypyrrole. *J. Appl. Phys.* **1998**, *83*, 3111-7. DOI
69. Du, Y.; Shen, S. Z.; Cai, K.; Casey, P. S. Research progress on polymer-inorganic thermoelectric nanocomposite materials. *Prog. Polym. Sci.* **2012**, *37*, 820-41. DOI
70. Chang, K.; Jeng, M.; Yang, C.; et al. The thermoelectric performance of poly(3,4-ethylenedi oxythiophene)/poly(4-styrenesulfonate) thin films. *J. Electron. Mater.* **2009**, *38*, 1182-8. DOI
71. Kim, D.; Kim, Y.; Choi, K.; Grunlan, J. C.; Yu, C. Improved thermoelectric behavior of nanotube-filled polymer composites with poly(3,4-ethylenedioxythiophene) poly(styrenesulfonate). *ACS. Nano.* **2010**, *4*, 513-23. DOI PubMed
72. Kim, G. H.; Shao, L.; Zhang, K.; Pipe, K. P. Engineered doping of organic semiconductors for enhanced thermoelectric efficiency. *Nat. Mater.* **2013**, *12*, 719-23. DOI
73. Culebras, M.; Gómez, C. M.; Cantarero, A. Enhanced thermoelectric performance of PEDOT with different counter-ions optimized by chemical reduction. *J. Mater. Chem. A.* **2014**, *2*, 10109-15. DOI
74. Park, Y. W.; Han, W. K.; Choi, C. H.; Shirakawa, H. Metallic nature of heavily doped polyacetylene derivatives: Thermopower. *Phys. Rev. B.* **1984**, *30*, 5847. DOI
75. Pukacki, W.; Płocharski, J.; Roth, S. Anisotropy of thermoelectric power of stretch-oriented new polyacetylene. *Synth. Met.* **1994**, *62*, 253-6. DOI
76. Lévesque, I.; Bertrand, P.; Blouin, N.; et al. Synthesis and thermoelectric properties of polycarbazole, polyindolocarbazole, and polydiindolocarbazole derivatives. *Chem. Mater.* **2007**, *19*, 2128-38. DOI
77. Feng-Xing, J.; Jing-Kun, X.; Bao-Yang, L.; Yu, X.; Rong-Jin, H.; Lai-Feng, L. Thermoelectric performance of poly(3,4-ethylenedioxythiophene): poly(styrenesulfonate). *Chinese. Phys. Lett.* **2008**, *25*, 2202. DOI
78. Scholdt, M.; Do, H.; Lang, J.; et al. Organic semiconductors for thermoelectric applications. *J. Electron. Mater.* **2010**, *39*, 1589-92. DOI
79. Sun, Y.; Wei, Z.; Xu, W.; Zhu, D. A three-in-one improvement in thermoelectric properties of polyaniline brought by nanostructures. *Synth. Met.* **2010**, *160*, 2371-6. DOI
80. Yoon, C.; Reghu, M.; Moses, D.; Cao, Y.; Heeger, A. Thermoelectric power of doped polyaniline near the metal-insulator transition. *Synth. Met.* **1995**, *69*, 273-4. DOI

81. Yakuphanoglu, F.; Şenkal, B. F.; Saraç, A. Electrical conductivity, thermoelectric power, and optical properties of organo-soluble polyaniline organic semiconductor. *J. Electron. Mater.* **2008**, *37*, 930-4. DOI
82. Wang, Z. H.; Scherr, E. M.; MacDiarmid, A. G.; Epstein, A. J. Transport and EPR studies of polyaniline: a quasi-one-dimensional conductor with three-dimensional "metallic" states. *Phys. Rev. B.* **1992**, *45*, 4190. DOI
83. Kemp, N. T.; Kaiser, A. B.; Trodahl, H. J.; et al. Effect of ammonia on the temperature-dependent conductivity and thermopower of polypyrrole. *J. Polym. Sci. B. Polym. Phys.* **2006**, *44*, 1331-8. DOI
84. Gao, X.; Uehara, K.; Klug, D. D.; Patchkovskii, S.; Tse, J. S.; Tritt, T. M. Theoretical studies on the thermopower of semiconductors and low-band-gap crystalline polymers. *Phys. Rev. B.* **2005**, *72*, 125202. DOI
85. Hiraishi, K.; Masuhara, A.; Nakanishi, H.; Oikawa, H.; Shinohara, Y. Evaluation of thermoelectric properties of polythiophene films synthesized by electrolytic polymerization. *Jpn. J. Appl. Phys.* **2009**, *48*, 071501. DOI
86. Yue, R.; Chen, S.; Lu, B.; Liu, C.; Xu, J. Facile electrosynthesis and thermoelectric performance of electroactive free-standing polythieno[3,2-b]thiophene films. *J. Solid. State. Electrochem.* **2011**, *15*, 539-48. DOI
87. Aïch, R. B.; Blouin, N.; Bouchard, A.; Leclerc, M. Electrical and thermoelectric properties of poly(2,7-carbazole) derivatives. *Chem. Mater.* **2009**, *21*, 751-7. DOI
88. Han Z, Fina A. Thermal conductivity of carbon nanotubes and their polymer nanocomposites: a review. *Prog. Polym. Sci.* **2011**, *36*, 914-44. DOI
89. Yu, C.; Kim, Y. S.; Kim, D.; Grunlan, J. C. Thermoelectric behavior of segregated-network polymer nanocomposites. *Nano. Lett.* **2008**, *8*, 4428-32. DOI
90. Hiroshige, Y.; Ookawa, M.; Toshima, N. High thermoelectric performance of poly(2,5-dimethoxyphenylenevinylene) and its derivatives. *Synth. Met.* **2006**, *156*, 1341-7. DOI
91. Wakim, S.; Aïch, B.; Tao, Y.; Leclerc, M. Charge transport, photovoltaic, and thermoelectric properties of poly(2,7-carbazole) and poly(indolo[3,2-*b*]carbazole) derivatives. *Polym. Rev.* **2008**, *48*, 432-62. DOI
92. Liu, H.; Wang, J.; Hu, X.; et al. Structure and electronic transport properties of polyaniline/$NaFe_4P_{12}$ composite. *Chem. Phys. Lett.* **2002**, *352*, 185-90. DOI
93. Park, H.; Lee, S. H.; Kim, F. S.; Choi, H. H.; Cheong, I. W.; Kim, J. H. Enhanced thermoelectric properties of PEDOT:PSS nanofilms by a chemical dedoping process. *J. Mater. Chem. A.* **2014**, *2*, 6532-9. DOI
94. Fan, Z.; Li, P.; Du, D.; Ouyang, J. Significantly enhanced thermoelectric properties of PEDOT:PSS films through sequential post-treatments with common acids and bases. *Adv. Energy. Mater.* **2017**, *7*, 1602116. DOI
95. Jung, I. H.; Hong, C. T.; Lee, U. H.; Kang, Y. H.; Jang, K. S.; Cho, S. Y. High thermoelectric power factor of a diketopyrrolopyrrole-based low bandgap polymer via finely tuned doping engineering. *Sci. Rep.* **2017**, *7*, 44704. DOI PubMed PMC
96. Liang, Z.; Zhang, Y.; Souri, M.; et al. Influence of dopant size and electron affinity on the electrical conductivity and thermoelectric properties of a series of conjugated polymers. *J. Mater. Chem. A.* **2018**, *6*, 16495-505. DOI
97. Liu, Z.; Hu, Y.; Li, P.; Wen, J.; He, J.; Gao, X. Enhancement of the thermoelectric performance of DPP based polymers by introducing one 3,4-ethylenedioxythiophene electron-rich building block. *J. Mater. Chem. C.* **2020**, *8*, 10859-67. DOI
98. Fei, Z.; Han, Y.; Gann, E.; et al. Alkylated selenophene-based ladder-type monomers via a facile route for high-performance thin-film transistor applications. *J. Am. Chem. Soc.* **2017**, *139*, 8552-61. DOI
99. Ashraf, R. S.; Meager, I.; Nikolka, M.; et al. Chalcogenophene comonomer comparison in small band gap diketopyrrolopyrrole-based conjugated polymers for high-performing field-effect transistors and organic solar cells. *J. Am. Chem. Soc.* **2015**, *137*, 1314-21. DOI
100. Wang, Z.; Liu, Z.; Ning, L.; et al. Charge mobility enhancement for conjugated DPP-selenophene polymer by simply replacing one bulky branching alkyl chain with linear one at each DPP unit. *Chem. Mater.* **2018**, *30*, 3090-100. DOI
101. Ding, J.; Liu, Z.; Zhao, W.; et al. Selenium-substituted diketopyrrolopyrrole polymer for high-performance p-type organic thermoelectric materials. *Angew. Chem. Int. Ed.* **2019**, *58*, 18994-9. DOI
102. Kim, N. Y.; Lee, T. S.; Lee, D. Y.; et al. Enhanced doping efficiency and thermoelectric performance of diketopyrrolopyrrole-based conjugated polymers with extended thiophene donors. *J. Mater. Chem. C.* **2021**, *9*, 340-7. DOI
103. Li, H.; Song, J.; Xiao, J.; Wu, L.; Katz, H. E.; Chen, L. Synergistically improved molecular doping and carrier mobility by copolymerization of donor-acceptor and donor-donor building blocks for thermoelectric application. *Adv. Funct. Mater.* **2020**, *30*, 2004378. DOI
104. Mao, X.; Li, X.; Zheng, D.; et al. Crystalline domain formation to enable high-performance polymer thermoelectrics inspired by thermocleavable materials. *ACS. Appl. Mater. Interfaces.* **2021**, *13*, 49348-57. DOI
105. Zhong, F.; Yin, X.; Chen, Z.; Gao, C.; Wang, L. Significantly reduced thermal-activation energy for hole transport via simple donor engineering: understanding the role of molecular parameters for thermoelectric behaviors. *ACS. Appl. Mater. Interfaces.* **2020**, *12*, 26276-85. DOI
106. Lee, T. S.; Lee, S. B.; Choi, D.; et al. Doping and thermoelectric behaviors of donor-acceptor polymers with extended planar backbone. *Macromol. Res.* **2021**, *29*, 887-94. DOI
107. Lee, H.; Li, H.; Kim, Y. S.; et al. Novel dithienopyrrole-based conjugated copolymers: importance of backbone planarity in achieving high electrical conductivity and thermoelectric performance. *Macromol. Rapid. Commun.* **2022**, *43*, 2200277. DOI
108. Suh, E. H.; Jeong, M.; Lee, K.; et al. Understanding the solution-state doping of donor-acceptor polymers through tailored side chain engineering for thermoelectrics. *Adv. Funct. Mater.* **2022**, *32*, 2207886. DOI
109. An, C.; Hou, J. Benzo[1,2-*b*:4,5-*b'*]dithiophene-based conjugated polymers for highly efficient organic photovoltaics. *Acc. Mater.*

Res. **2022**, *3*, 540-51. DOI

110. Li, B.; Li, X.; Yang, F.; et al. Enhanced thermoelectric performance of a donor-acceptor-based two-dimensional conjugated polymer with high crystallinity. *ACS. Appl. Energy. Mater.* **2021**, *4*, 4662-71. DOI
111. Cao, G.; Li, B.; Wu, Y.; et al. Alleviating the trade-off interrelation between seebeck coefficient and electrical conductivity by random copolymerization of two-dimensional and one-dimensional monomers. *Compos. Commun.* **2022**, *33*, 101218. DOI
112. Lee, H.; Ayuningtias, L.; Kim, H.; et al. From non-doped to dopable: the impact of methoxy functionalization on doping and thermoelectric properties of conjugated polymers. *EcoMat* **2024**, *6*, e12442. DOI
113. Kim, S. B.; Song, S.; Lee, T. S.; et al. Influence of the electronic structures of diketopyrrolopyrrole-based donor-acceptor conjugated polymers on thermoelectric performance. *J. Mater. Chem. C.* **2024**, *12*, 9227-35. DOI
114. Mun, J.; Wang, G. N.; Oh, J. Y.; et al. Effect of nonconjugated spacers on mechanical properties of semiconducting polymers for stretchable transistors. *Adv. Funct. Mater.* **2018**, *28*, 1804222. DOI
115. Galuska, L. A.; Mcnutt, W. W.; Qian, Z.; et al. Impact of backbone rigidity on the thermomechanical properties of semiconducting polymers with conjugation break spacers. *Macromolecules* **2020**, *53*, 6032-42. DOI
116. Lin, Y.; Matsuda, M.; Chen, C.; et al. Investigation of the mobility-stretchability properties of naphthalenediimide-based conjugated random terpolymers with a functionalized conjugation break spacer. *Macromolecules* **2021**, *54*, 7388-99. DOI
117. Liu, D.; Mun, J.; Chen, G.; et al. A design strategy for intrinsically stretchable high-performance polymer semiconductors: incorporating conjugated rigid fused-rings with bulky side groups. *J. Am. Chem. Soc.* **2021**, *143*, 11679-89. DOI
118. Liu, D.; Lei, Y.; Ji, X.; et al. Tuning the mechanical and electric properties of conjugated polymer semiconductors: side-chain design based on asymmetric benzodithiophene building blocks. *Adv. Funct. Mater.* **2022**, *32*, 2203527. DOI
119. Tseng, C. C.; Wang, K. C.; Lin, P. S.; et al. Intrinsically stretchable organic thermoelectric polymers enabled by incorporating fused-ring conjugated breakers. *Small* **2024**, *20*, 2401966. DOI
120. Zeng, Y.; Zheng, W.; Guo, Y.; Han, G.; Yi, Y. Doping mechanisms of N-DMBI-H for organic thermoelectrics: hydrogen removal *vs.* hydride transfer. *J. Mater. Chem. A.* **2020**, *8*, 8323-8. DOI
121. Ma, W.; Shi, K.; Wu, Y.; et al. Enhanced molecular packing of a conjugated polymer with high organic thermoelectric power factor. *ACS. Appl. Mater. Interfaces.* **2016**, *8*, 24737-43. DOI
122. Feng, K.; Guo, H.; Wang, J.; et al. Cyano-Functionalized bithiophene imide-based n-type polymer semiconductors: synthesis, structure-property correlations, and thermoelectric performance. *J. Am. Chem. Soc.* **2021**, *143*, 1539-52. DOI
123. Yan, X.; Xiong, M.; Li, J. T.; et al. Pyrazine-flanked diketopyrrolopyrrole (DPP): a new polymer building block for high-performance n-type organic thermoelectrics. *J. Am. Chem. Soc.* **2019**, *141*, 20215-21. DOI
124. Han, J.; Chiu, A.; Ganley, C.; et al. 3,4,5-trimethoxy substitution on an N-DMBI Dopant with new N-type polymers: polymer-dopant matching for improved conductivity-seebeck coefficient relationship. *Angew. Chem. Int. Ed.* **2021**, *60*, 27212-9. DOI
125. Lu, Y.; Wang, J.; Pei, J. Strategies to enhance the conductivity of n-type polymer thermoelectric materials. *Chem. Mater.* **2019**, *31*, 6412-23. DOI
126. Sun, Y.; Di, C.; Xu, W.; Zhu, D. Advances in n-type organic thermoelectric materials and devices. *Adv. Elect. Mater.* **2019**, *5*, 1800825. DOI
127. Nicolai, H. T.; Kuik, M.; Wetzelaer, G. A.; et al. Unification of trap-limited electron transport in semiconducting polymers. *Nat. Mater.* **2012**, *11*, 882-7. DOI
128. Leeuw D, Simenon M, Brown A, Einerhand R. Stability of n-type doped conducting polymers and consequences for polymeric microelectronic devices. *Synth. Met.* **1997**, *87*, 53-9. DOI
129. Wang, S.; Sun, H.; Ail, U.; et al. Thermoelectric properties of solution-processed n-doped ladder-type conducting polymers. *Adv. Mater.* **2016**, *28*, 10764-71. DOI
130. Naab, B. D.; Gu, X.; Kurosawa, T.; To, J. W. F.; Salleo, A.; Bao, Z. Role of polymer structure on the conductivity of N-doped polymers. *Adv. Electron. Mater.* **2016**, *2*, 1600004. DOI
131. Liu, J.; Qiu, L.; Alessandri, R.; et al. Enhancing molecular n-type doping of donor-acceptor copolymers by tailoring side chains. *Adv. Mater.* **2018**, *30*, 1704630. DOI
132. Wang, Y.; Yang, L.; Shi, X. L.; et al. Flexible thermoelectric materials and generators: challenges and innovations. *Adv. Mater.* **2019**, *31*, 1807916. DOI
133. Yang, C. Y.; Jin, W. L.; Wang, J.; et al. Enhancing the n-type conductivity and thermoelectric performance of donor-acceptor copolymers through donor engineering. *Adv. Mater.* **2018**, *30*, 1802850. DOI
134. Wang, Y.; Takimiya, K. Naphthodithiophenediimide-bithiopheneimide copolymers for high-performance n-type organic thermoelectrics: significant impact of backbone orientation on conductivity and thermoelectric performance. *Adv. Mater.* **2020**, *32*, e2002060. DOI PubMed
135. Wang, S.; Sun, H.; Erdmann, T.; et al. A chemically doped naphthalenediimide-bithiazole polymer for n-type organic thermoelectrics. *Adv. Mater.* **2018**, *30*, 1801898. DOI
136. Wang, S.; Fazzi, D.; Puttisong, Y.; et al. Effect of backbone regiochemistry on conductivity, charge density, and polaron structure of n-doped donor-acceptor polymers. *Chem. Mater.* **2019**, *31*, 3395-406. DOI
137. Tripathi, A.; Lee, Y.; Lee, S.; Woo, H. Y. Recent advances in n-type organic thermoelectric materials, dopants, and doping strategies. *J. Mater. Chem. C.* **2022**, *10*, 6114-40. DOI
138. Lu, Y.; Yu, Z. D.; Un, H. I.; et al. Persistent conjugated backbone and disordered lamellar packing impart polymers with efficient n-

doping and high conductivities. *Adv. Mater.* **2021**, *33*, 2005946. DOI

139. Liu, J.; Shi, Y.; Dong, J.; et al. Overcoming coulomb interaction improves free-charge generation and thermoelectric properties for n-doped conjugated polymers. *ACS. Energy. Lett.* **2019**, *4*, 1556-64. DOI
140. Guo, H.; Yang, C. Y.; Zhang, X.; et al. Transition metal-catalysed molecular n-doping of organic semiconductors. *Nature* **2021**, *599*, 67-73. DOI
141. Yan, H.; Chen, Z.; Zheng, Y.; et al. A high-mobility electron-transporting polymer for printed transistors. *Nature* **2009**, *457*, 679-86. DOI
142. Guo, K.; Bai, J.; Jiang, Y.; et al. Diketopyrrolopyrrole-based conjugated polymers synthesized via direct arylation polycondensation for high mobility pure n-channel organic field-effect transistors. *Adv. Funct. Mater.* **2018**, *28*, 1801097. DOI
143. Park, J. H.; Jung, E. H.; Jung, J. W.; Jo, W. H. A fluorinated phenylene unit as a building block for high-performance n-type semiconducting polymer. *Adv. Mater.* **2013**, *25*, 2583-8. DOI PubMed
144. Sun, B.; Hong, W.; Yan, Z.; Aziz, H.; Li, Y. Record high electron mobility of 6.3 $cm^2 V^{-1} s^{-1}$ achieved for polymer semiconductors using a new building block. *Adv. Mater.* **2014**, *26*, 2636-42. DOI PubMed
145. Yan, X.; Xiong, M.; Deng, X. Y.; et al. Approaching disorder-tolerant semiconducting polymers. *Nat. Commun.* **2021**, *12*, 5723. DOI PubMed PMC
146. Wang, J.; Feng, K.; Jeong, S. Y.; et al. Acceptor-acceptor type polymers based on cyano-substituted benzochalcogenadiazole and diketopyrrolopyrrole for high-efficiency n-type organic thermoelectrics. *Polym. J.* **2023**, *55*, 507-15. DOI
147. Shi, Y.; Zhang, X.; Du, T.; Han, Y.; Deng, Y.; Geng, Y. A high-performance n-type thermoelectric polymer from C-H/C-H oxidative direct arylation polycondensation. *Angew. Chem. Int. Ed.* **2023**, *62*, e202219262. DOI
148. Tu, L.; Wang, J.; Wu, Z.; et al. Cyano-functionalized pyrazine: a structurally simple and easily accessible electron-deficient building block for n-type organic thermoelectric polymers. *Angew. Chem. Int. Ed.* **2024**, *63*, e202319658. DOI
149. Gao, Y.; Ke, Y.; Wang, T.; et al. An n-type conjugated polymer with low crystallinity for high-performance organic thermoelectrics. *Angew. Chem. Int. Ed.* **2024**, *63*, e202402642. DOI
150. Shen, T.; Liu, D.; Zhang, J.; Wei, Z.; Wang, Y. A high-mobility n-type noncovalently-fused-ring polymer for high-performance organic thermoelectrics. *Angew. Chem. Int. Ed.* **2024**, *63*, e202409018. DOI
151. Ma, M.; Ye, G.; Jang, S.; et al. Realizing an N-type organic thermoelectric ZT of 0.46. *ACS. Energy. Lett.* **2025**, *10*, 1813-20. DOI
152. Tripathi, A.; Ko, Y.; Kim, M.; et al. Optimization of thermoelectric properties of polymers by incorporating oligoethylene glycol side chains and sequential solution doping with preannealing treatment. *Macromolecules* **2020**, *53*, 7063-72. DOI
153. Lee, Y.; Park, J.; Son, J.; Woo, H. Y.; Kwak, J. Degenerately doped semi-crystalline polymers for high performance thermoelectrics. *Adv. Funct. Mater.* **2021**, *31*, 2006900. DOI
154. Yoon, S. E.; Kang, Y.; Noh, S. Y.; et al. High efficiency doping of conjugated polymer for investigation of intercorrelation of thermoelectric effects with electrical and morphological properties. *ACS. Appl. Mater. Interfaces.* **2020**, *12*, 1151-8. DOI
155. Jacobs, I. E.; Aasen, E. W.; Oliveira, J. L.; et al. Comparison of solution-mixed and sequentially processed P3HT:F4TCNQ films: effect of doping-induced aggregation on film morphology. *J. Mater. Chem. C.* **2016**, *4*, 3454-66. DOI
156. Fontana, M. T.; Stanfield, D. A.; Scholes, D. T.; Winchell, K. J.; Tolbert, S. H.; Schwartz, B. J. Evaporation vs solution sequential doping of conjugated polymers: F_4TCNQ doping of micrometer-thick P3HT films for thermoelectrics. *J. Phys. Chem. C.* **2019**, *123*, 22711-24. DOI
157. Ma, T.; Dong, B. X.; Onorato, J. W.; et al. Correlating conductivity and Seebeck coefficient to doping within crystalline and amorphous domains in poly(3-(methoxyethoxyethoxy)thiophene). *J. Polym. Sci.* **2021**, *59*, 2797-808. DOI
158. Karpov, Y.; Erdmann, T.; Stamm, M.; et al. Molecular doping of a high mobility diketopyrrolopyrrole-dithienylthieno[3,2-*b*]thiophene donor-acceptor copolymer with F6TCNNQ. *Macromolecules* **2017**, *50*, 914-26. DOI
159. Kroon, R.; Kiefer, D.; Stegerer, D.; Yu, L.; Sommer, M.; Müller, C. Polar side chains enhance processability, electrical conductivity, and thermal stability of a molecularly p-doped polythiophene. *Adv. Mater.* **2017**, *29*, 1700930. DOI PubMed
160. Karpov, Y.; Erdmann, T.; Raguzin, I.; et al. High conductivity in molecularly p-doped diketopyrrolopyrrole-based polymer: the impact of a high dopant strength and good structural order. *Adv. Mater.* **2016**, *28*, 6003-10. DOI
161. Saska, J.; Gonel, G.; Bedolla-valdez, Z. I.; et al. A freely soluble, high electron affinity molecular dopant for solution processing of organic semiconductors. *Chem. Mater.* **2019**, *31*, 1500-6. DOI
162. Patel, S. N.; Glaudell, A. M.; Kiefer, D.; Chabinyc, M. L. Increasing the thermoelectric power factor of a semiconducting polymer by doping from the vapor phase. *ACS. Macro. Lett.* **2016**, *5*, 268-72. DOI PubMed
163. Schlitz, R. A.; Brunetti, F. G.; Glaudell, A. M.; et al. Solubility-limited extrinsic n-type doping of a high electron mobility polymer for thermoelectric applications. *Adv. Mater.* **2014**, *26*, 2825-30. DOI
164. Un, H.; Gregory, S. A.; Mohapatra, S. K.; et al. Understanding the effects of molecular dopant on n-type organic thermoelectric properties. *Adv. Energy. Mater.* **2019**, *9*, 1900817. DOI
165. Dong, C.; Deng, S.; Meng, B.; Liu, J.; Wang, L. A Distannylated monomer of a strong electron-accepting organoboron building block: enabling acceptor-acceptor-type conjugated polymers for n-type thermoelectric applications. *Angew. Chem. Int. Ed.* **2021**, *60*, 16184-90. DOI
166. Wang, S.; Ruoko, T. P.; Wang, G.; et al. Sequential doping of ladder-type conjugated polymers for thermally stable n-type organic conductors. *ACS. Appl. Mater. Interfaces.* **2020**, *12*, 53003-11. DOI PubMed PMC
167. Zhang, F.; Zang, Y.; Huang, D.; et al. Modulated thermoelectric properties of organic semiconductors using field-effect transistors.

Adv. Funct. Mater. **2015**, *25*, 3004-12. DOI

168. Rossi, P.; Pallini, F.; Coco, G.; et al. An iminostilbene functionalized benzimidazoline for enhanced n-type solution doping of semiconducting polymers for organic thermoelectrics. *Adv. Mater. Interfaces.* **2023**, *10*, 2202416. DOI
169. Huang, D.; Yao, H.; Cui, Y.; et al. Conjugated-backbone effect of organic small molecules for n-type thermoelectric materials with ZT over 0.2. *J. Am. Chem. Soc.* **2017**, *139*, 13013-23. DOI
170. Naab, B. D.; Guo, S.; Olthof, S.; et al. Mechanistic study on the solution-phase n-doping of 1,3-dimethyl-2-aryl-2,3-dihydro-1H-benzoimidazole derivatives. *J. Am. Chem. Soc.* **2023**, *135*, 15018-25. DOI